GEOLOGICA CARPATHICA, APRIL 2018, 69, 2, 169–186 doi: 10.1515/geoca-2018-0010

New results of microfaunal and geochemical investigations in the Permian–Triassic boundary interval from the Jadar Block (NW Serbia)

MILAN N. SUDAR[1,✉], TEA KOLAR-JURKOVŠEK[2], GALINA P. NESTELL[3], DIVNA JOVANOVIĆ[4], BOGDAN JURKOVŠEK[2], JEREMY WILLIAMS[5], MICHAEL BROOKFIELD[6] and ALAN STEBBINS[6]

[1]Serbian Academy of Sciences and Arts, Knez Mihaila 35, 11000 Belgrade, Serbia; ✉milan.sudar1946@gmail.com
[2]Geological Survey of Slovenia, Dimičeva 14, 1000 Ljubljana, Slovenia
[3]Department of Earth and Environmental Sciences, University of Texas at Arlington, Arlington, TX 76019, USA; Faculty of Geology, St. Petersburg State University, St. Petersburg, Russia
[4]Geological Survey of Serbia, Rovinjska 12, 11000 Belgrade, Serbia
[5]Department of Geology, Kent State University, Kent, OH 44242, USA
[6]School for the Environment, University of Massachusetts at Boston, 100 Morrissey Blvd. Boston, MA 02125, USA

(Manuscript received September 28, 2017; accepted in revised form February 12, 2018)

Abstract: Detail results of microfaunal, sedimentological and geochemical investigations are documented from a newly discovered section of the Permian–Triassic boundary (PTB) interval in the area of the town of Valjevo (northwestern Serbia). The presence of various and abundant microfossils (conodonts, foraminifers, and ostracodes) found in the Upper Permian "Bituminous limestone" Formation enabled a determination of the Changhsingian *Hindeodus praeparvus* conodont Zone. This paper is the first report of latest Permian strata from the region, as well as from all of Serbia, where the PTB interval sediments have been part of a complex/integrated study by means of biostratigraphy and geochemistry.

Keywords: Conodonts, *Hindeodus praeparvus* Zone, foraminifers, C–N–S isotopes, northwestern Palaeotethys.

Introduction

Permian and Triassic deposits are widespread in the Jadar Block in NW Serbia and their specific palaeontological and lithological/sedimentological characteristics are unique in Serbia. Therefore, they have been the subject of intensive geological studies. Generally, Upper Permian shallow-water marine carbonate rocks contain diverse and very rich macro- and micro-biocenoses (without ammonoids, but with brachiopods, bivalves, gastropods, algae, and foraminifers), whereas in the Lower Triassic sediments fossil associations are rather poor and are represented by rare molluscs, foraminifers and ostracodes.

During numerous field investigations for this study in the Jadar Block (NW Serbia), the Serbian and Slovenian authors of this paper intended to document new geological data to refine existing stratigraphical, lithostratigraphical and sedimentological determinations. Then, special attention was initiated for the purpose of establishing reference sections of the PTB interval in this area of Serbia. These investigations started in 2005, and until now their results have been published in Sudar et al. (2007), Nestell et al. (2009), Crasquin et al. (2010), and Sudar et al. (2014).

The aim of this paper is to confirm the presence of microfossils and to present the results of a biostratigraphical, sedimentological and geochemical study of the continuous carbonate sedimentary succession from the Upper Permian to the Lower Triassic in the Sitarička Glavica section in the vicinity of Valjevo (Jadar Block, NW Serbia) (Fig. 1).

Geological setting

During the Permian–Triassic, the investigated Serbian PTB Sitarička Glavica section was situated palaeogeographicaly in the northwestern Palaeotethys along the passive margin of Pangea (Schobben et al. 2014) (Fig. 1A). At the present time, the Jadar Block is located at the southern margin of the Pannonian Basin and belongs to the central part of the Balkan Peninsula. It occupies a large part of northwestern Serbia, southern Srem (Vojvodina) and partly extends westward over the Drina River into eastern Bosnia (Fig. 1B).

The Jadar Block unit is today an exotic block emplaced into the Vardar Zone before the Late Cretaceous. It is surrounded by the Vardar Zone Western Belt, except on the farthest southeastern part where it is in direct contact with the Kopaonik Block and the Ridge Unit (Fig. 1B). The Jadar Block differs from the Vardar Zone Western Belt in lacking post-Liassic sediments as well as in the absence of ultramafites, ophiolitic melange, and Cretaceous flysch development (Filipović et al. 2003).

In the investigated area, deposition occurred during the Variscan and Early Alpine evolution with a domination of

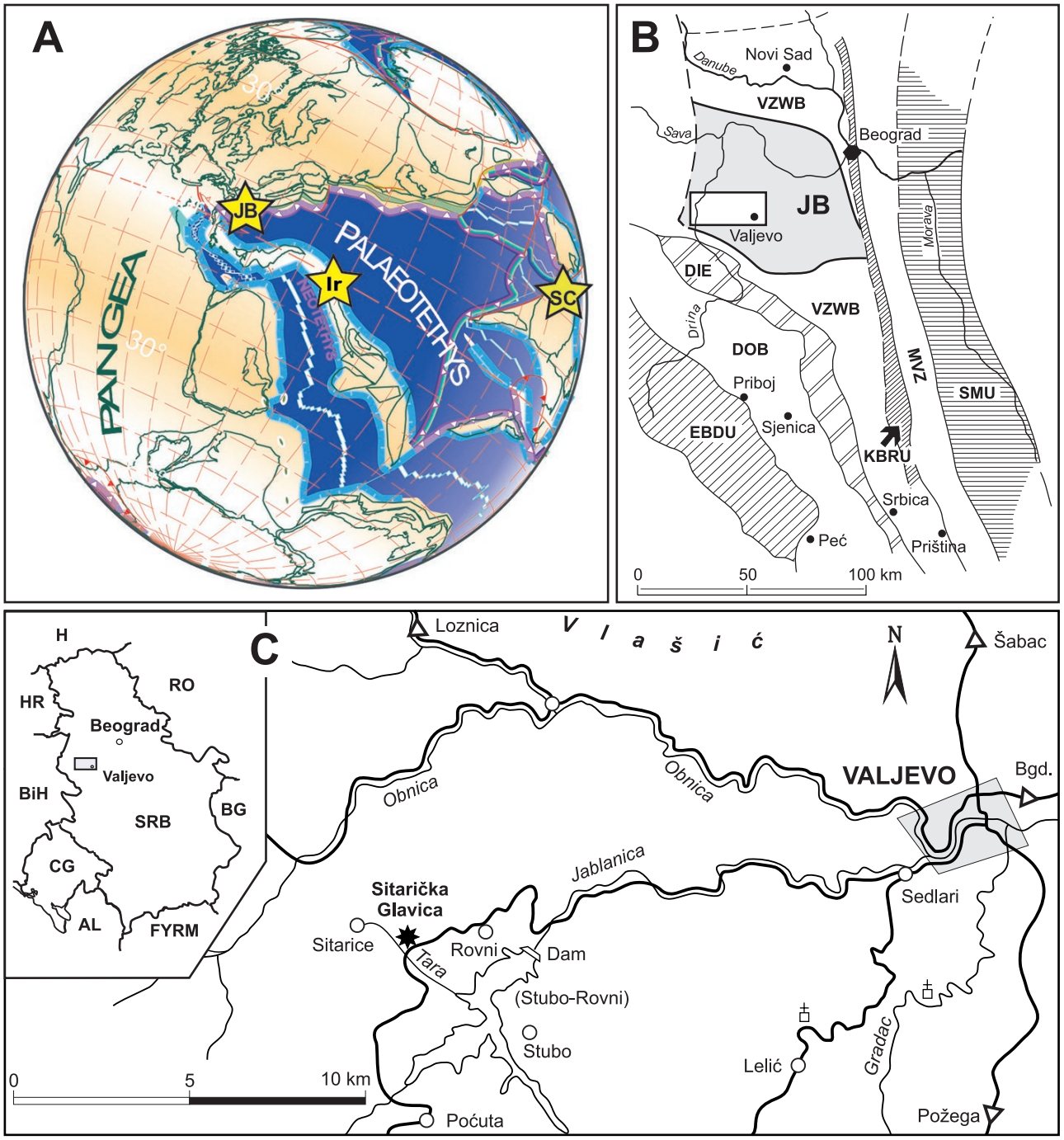

Fig. 1. Locations of the Jadar Block (NW Serbia) and Sitarička Glavica section: **A** — Palaeogeography during the PTB interval with the location of the next sections: JB — Jadar Block in NW Serbia; Ir — NW Iran and SC — South China (adapted and modified from Schobben et al. 2014). **B** — Terranes of a part of the Balkan Peninsula (Karamata et al. 2000; Karamata 2006): SMU — Serbian-Macedonian Unit; MVZ — Main Vardar Zone; KBRU — Kopaonik Block and the Ridge Unit; VZWB — Vardar Zone Western Belt; JB — Jadar Block; DIE — Drina–Ivanjica Element; DOB — Dinaridic Ophiolite Belt and EBDU — East Bosnian-Durmitor Unit (modified after Sudar et al. 2014). **C** – Geographic position of the Sitarička Glavica section in the south-western part of Jadar Block (NW Serbia): SRB — Serbia; H — Hungary; RO — Romania; BG — Bulgaria; FYRM — Former Yugoslav Republic of Macedonia; AL — Albania; CG — Crna Gora (Montenegro); BiH — Bosnia and Herzegovina; HR — Hrvatska (Croatia).

Dinaridic features. The later tectonic stage is characterized by the sedimentation of the Upper Permian and lowermost Triassic shallow-water marine carbonate, Anisian dolomite, Ladinian "porphyrite" and pyroclastic rocks, Middle and Upper Triassic platform-reefal limestone and a gradual transition into Lower Jurassic limestone.

In the Jadar Block, the Upper Permian is represented by the "Bituminous limestone" Formation, and the lower part of

the Lower Triassic belongs to the Svileuva Formation (Filipović et al. 2003). They are both time equivalent with formations of the Southern Carnic Alps, the first one with the Bellerophon Formation, and the second one with the lower part of the Werfen Formation.

Materials and methods

For the purpose of this study, a total of 26 samples were processed for conodonts and making of thin sections. During the field work in 2012, 19 composite samples for conodonts were collected and only one of them (KM4) was productive. Therefore, this level was resampled in detail in 2013 when seven additional samples were collected and all of them turned out to contain conodonts. The stratigraphic position of the samples is presented in Figs. 2, 3.

The laboratory preparation of the samples were carried out at Geological Survey of Slovenia (GeoZS), Ljubljana where all micropalaeontological and sedimentological materials are stored and inventoried under the repository numbers 5088–5102 and 5328–5334 and abbreviated GeoZS. The standard technique to process conodont samples with the use of dilute acetic acid was applied and followed by heavy liquid separation. The illustrated conodont elements presented herein were photographed using the JEOL JSM 6490LV Scanning Electron Microscope at the Geological Survey of Slovenia. The microphotographs of foraminifers were taken in the Department of Earth and Environmental Sciences, University of Texas at Arlington, Arlington, USA. Scanning electron microscope images of framboidal pyrite were obtained from the University of Massachusetts Boston Environmental Analytical Facilitites, USA.

The Sitarička Glavica section

The Sitarička Glavica section contains a newly discovered PTB interval exposed along the road Valjevo-Poćuta (Bajina Bašta) near the dam Stubo-Rovni, about 100 km SW from Belgrade and 14 km WSW of the town of Valjevo (N 44º14'33.8", E 19º43'20.3") (Fig. 1C). The section is located near the village of Sitarice just before the bridge over the Tara River, a small tributary of the Jablanica River. At the beginning of our investigations this section was named Krivi Most (abbreviation for samples=KM).

Detail field investigations of the joint Serbian–Slovenian research team of geologists (M. Sudar, D. Jovanović, T. Kolar-Jurkovšek, and B. Jurkovšek) were done in 2012, 2013 and 2016. The entire studied section is over 50 meters thick and consists of mostly tectonized Upper Permian and Lower Triassic sediments of which only a 17.74 m thick interval not disrupted by a shear zone was sampled for microfaunal and sedimentological investigations (Figs. 2, 3).

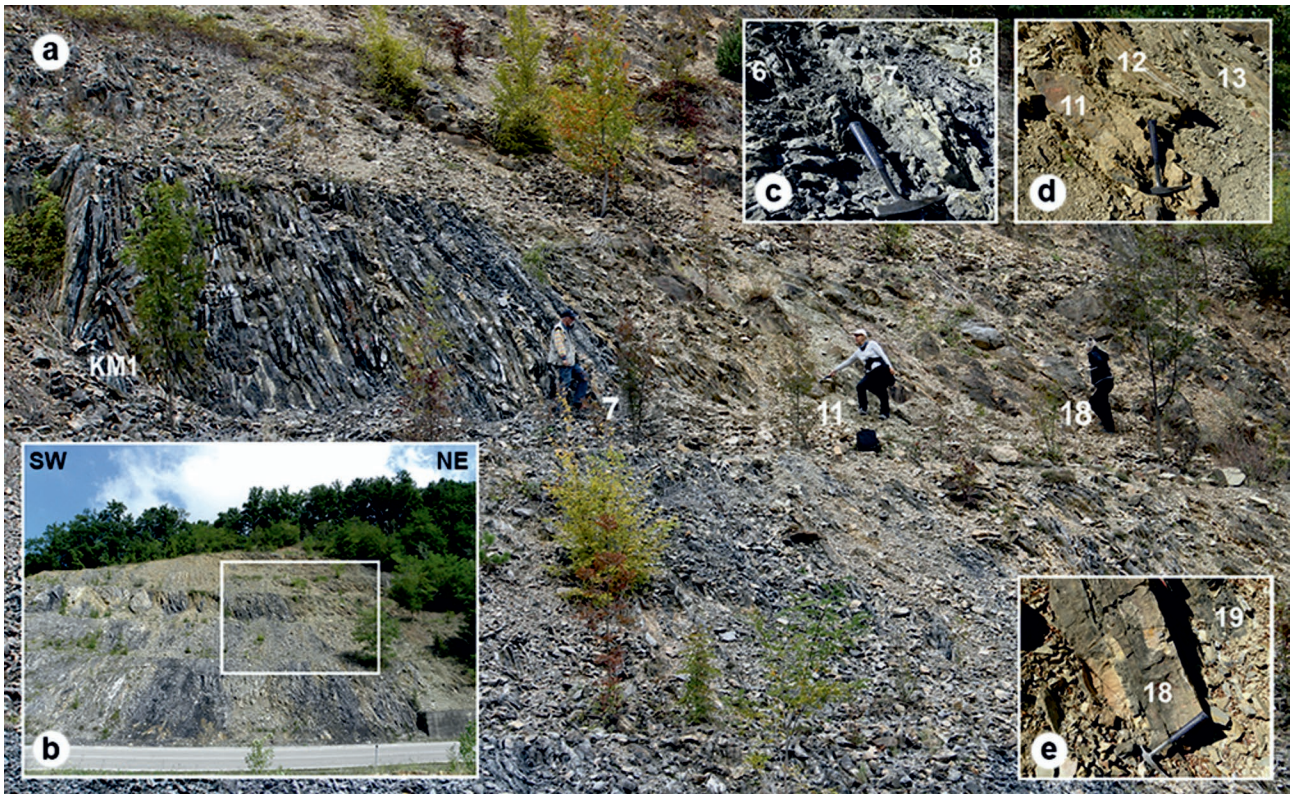

Fig. 2. a — Sitarička Glavica section; **b** — panoramic view of Sitarička Glavica section; **c**–**e** — positions of samples KM7 (**c**), KM11 (**d**) and KM18 (**e**).

Lithology and sedimentology

The Sitarička Glavica section is subdivided into two parts, i.e. into four units according to field investigations based on macroscopic (lithologic) characteristics, and later by detailed sedimentological and micropalaeontological studies.

The lower part, Unit 1, 7.22 m thick, is represented by black and dark grey thick- to thin-bedded bituminous, predominantly nodular limestone (wackestone, very rare mudstone) intercalated rarely with very thin layers of calcisiltite and limy shale. The rocks of the following units, 2 (2.22 m), 3 (7.37 m) and 4 (0.95 m), are different in lithology from the lower unit, and are much lighter in colour with the prevalence of light grey, yellow and almost brown shades. Also, sandy and micaceous components in the upper part are typical (Fig. 2).

Unit 1 (samples KM1–KM7) contains an abundant partly fragmented macrofauna (brachiopods, gastropods, bivalves, different parts of echinodermates, etc.) and microfossils (algae, foraminifers, conodonts, ostracodes). Unit 2 (samples KM8–KM11) contains similar macro- and microfossils as are found in Unit 1, but are not as abundant. The fossils are much more fragmented, and in comparison with Unit 1 that had rich foraminiferal assemblages, only a few species survived in Unit 2. The second part of the section beginning with Unit 3 (samples KM12–KM17) and then Unit 4 (samples KM18, KM19) differs from the previous two units in very poor fossil content yielding no foraminifers, but only fragments of molluscs (bivalves, gastropods) and rare accumulations of bivalves.

The lowermost part of the section (1.0 m; sample KM1) is represented by silty wackestone. Its main characteristic is the abundance of biodetritus comprising fragments of algae, echinoids, and gastropods. The lower part of the following 2.27 m (samples KM2, KM3) is represented by wackestone, party recrystallized, with abundant small foraminifers of various species. Calcite veinlets, silty quartz and sericite, fine organic matter are typical as well as fragments of algae and other fauna. Very similar biodetritus is also present upward in the mudstone, but foraminifers are less frequent and not diverse. The next 2.40 m (samples KM4, KM5) are dark grey, weakly laminated bioclastic wackestone. Due to the presence of the Late Permian conodonts, the bed, first marked only as KM4, was later studied in detail (samples KM4A–KM4G). Together with the conodonts, numerous parallel oriented fragments of macro- and microfossils (gastropods, brachiopods, crinoids, echinoids, and algae) and diverse foraminiferal species are present. Very interesting and important is also the appearance of four taxa of fusulinaceans which are not often found in Upper Permian sediments in the Jadar Block area. Upward (sample KM5) follows a bioclastic wackestone that contains predominantly bivalves with thin and thick shells, and rare foraminifers. This Unit passes into dark grey to black coloured thin-bedded, laminated nodular bioclastic wackestone (sample KM6), partly intercalated with grey calcisiltite and limy shale. The final part of Unit 1 is topped by a 60 cm thick bed of dark grey calcisiltite and limy shale. One layer of nodular clayey limestone (sample KM7) with similar biodetritus as in the previous strata is present in this bed.

Unit 2, 2.20 m thick (samples KM8 to KM11), which conditionally could represents the "transitional beds" toward the Lower Triassic sediments, is still in the Upper Permian part of the section. Unit 2 is similar in lithology with the previous Unit 1 and is represented by thin-bedded silty–clayey bioclastic wackestone intercalated with mm-cm thick calcisiltite and limy shale. Siliciclastic detritus is mostly parallel and weakly wavy oriented. Moreover, also an unequally/irregularly fragmented macro- and microfauna both exhibit stratification. Small foraminifers are scarce, however, they are of Late Permian (Changhsingian) age (Fig. 3). Some of them are replaced by silica or marked with fine organic matter. Algae are very abundant and deformed. In the uppermost part of this Unit abundant and different shell fragments are larger than in the previous layers. Rare microfissures are filled with organic matter.

The prevalence of bioclastic silty–clayey wackestone in the lower part of the section (units 1 and 2), and the presence of abundant small foraminifers, especially hemigordiopsids, are usual for deposition under low energy conditions in a partly restricted, very shallow water environment. Abundant biodetritus (gastropods, brachiopods, crinoid ossicles, parts of echinoids, and algae) indicate back-reefal (lagoonal) origin. Siliciclastic imput such as silty quartz, sericite, and fine organic matter also suggests a very shallow environment. These constituents are typical for Upper Permian Changhsingian strata known from different regions of the Palaeotethys (Korte & Kozur 2010; Kolar-Jurkovšek et al. 2011a, b; Farabegoli & Perri 2012).

In the interval of the section named as the "transitional beds" (Unit 2) marine conditions obviously were changed. In a partly restricted, shallow water environment some local tectonic movements (presence of fragmented macro- and microfauna) and weak oscillatory currents (wavy structure) occurred. Only some rare species of Late Permian foraminifers survived in the transitional interval. This diminishment of species could be explained with the beginning of mass extinction which continued gradually (Fig. 3).

The upper part of the sampled section is first represented by Unit 3 (7.37 m) that consists of thin-bedded sandy, silty–clayey limestone, and micaceous biomicrosparite frequently interbedded with micaceous siltstone (shale) (samples from KM12 to KM17). The limestone is mostly parallel laminated and weakly graded. Occasionally it contains concentrations of sparitic shell fragments of bivalves that exhibit stratification (sample KM14). Sporadically there appears thin (less than 1 mm) parallel concentrations of siliciclastic detritus: fine sandy/silty quartz grains and sericite with submm-thin ferruginous rhomboidal calcite concentrations. Dolomite is rare and numerous calcite veins cut the rock. Sample KM17 represents a coquina with very frequent small indeterminable bivalve shells.

The last Unit 4 (0.95 m) starts with bedded sparitic limestone–ooidal grainstone (sample KM18). Ooids are simple

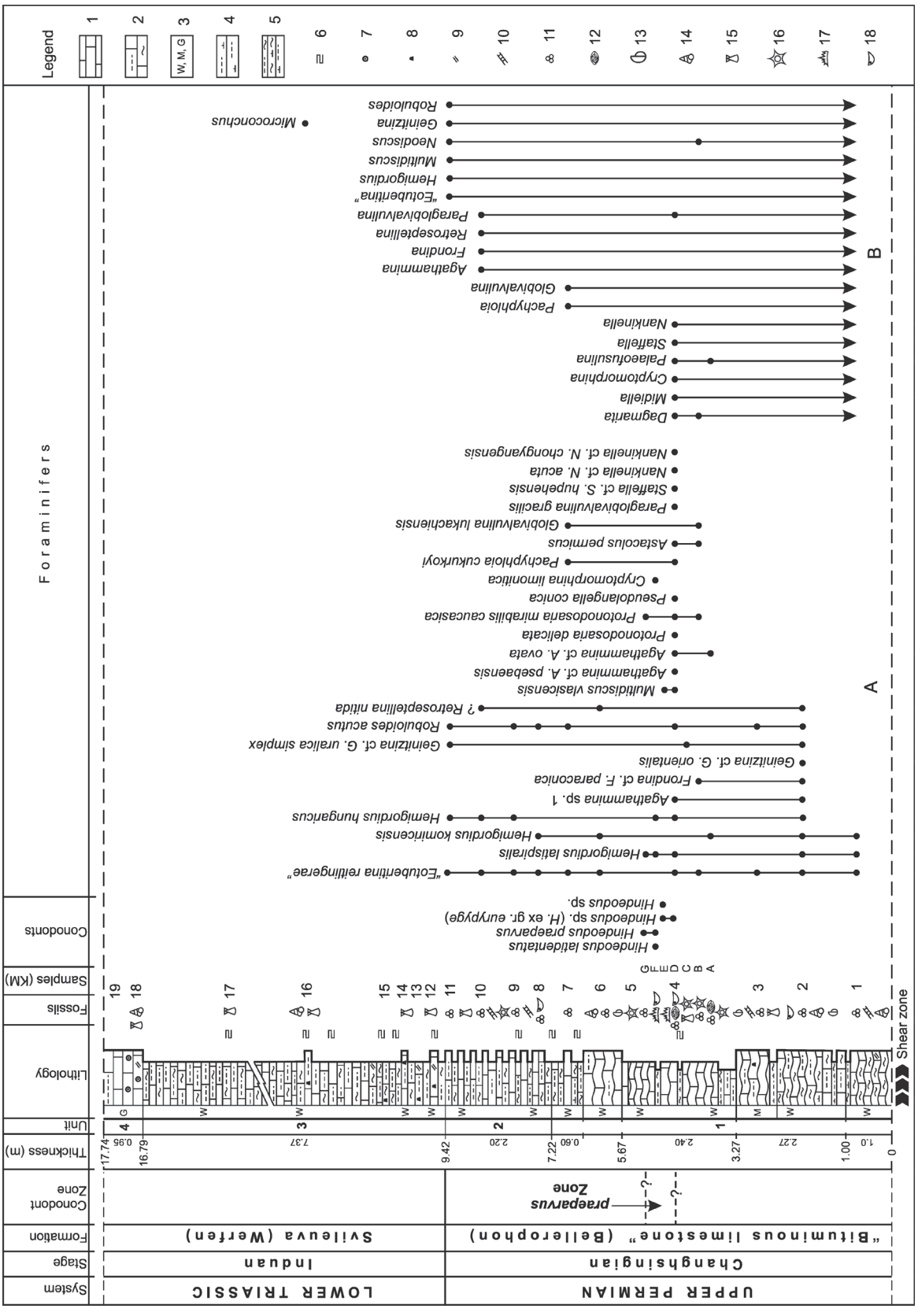

Fig. 3. Geological column, conodont stratigraphic ranges and zone, distribution of the species of foraminifers (**A**) and the last appearance of their genera (**B**) with the appearance of the genus *Microconchus* in the Sitarička Glavica section, Jadar Block, NW Serbia. Legend: 1 — limestone; 2 — silty-clayey limestone; 3 — limestone types: W — wackestone, M — mudstone, G — grainstone; 4 — limy siltstone; 5 — calcisiltite and limy shale; 6 — parallel lamination; 7 — ooids; 8 — ferruginous matter; 9 — mica; 10 — algae; 11 — small foraminifers; 12 — fusulinaceans; 13 — brachiopods; 14 — gastropods; 15 — bivalves; 16 — echinoderms (crinoid ossicles, holothurian sclerites, and parts of echinoids); 17 — conodonts; 18 — ostracodes.

with one, rare two or three, superficial cortex, filled with sparite. They are usually flattened, marked with fine ferruginous matter. Fragments of recrystallized shells are rare. The final part of the section (sample KM19) is represented by calcisiltite and limy shale with small amounts of silty quartz, sericite and organic matter.

The sediments of the terminal part of the section were deposited on a wider area in a shallow epeiric shelf of ramp with very low slope angle. Due to occasional tidal currents and higher water energy ooidal grainstone was formed. The grainstone is followed by concentrations of shell fragments which alternate with siliciclastic (sandy, silty) concentrations.

Chronostratigraphy, biostratigraphy and the Permian–Triassic boundary

Upper Permian and Lower Triassic sediments are recognized in the Sitarička Glavica section. A Changhsingian, latest Permian conodont *Hindeodus praeparvus* Zone has been identified within the lower part of the section (units 1 and 2) on the basis of very diverse and abundant fossil associations, especially biostratigraphic characteristics of conodonts and foraminifers. The sediments of this part of the section belong to the "Bituminous limestone" (Bellerophon) Formation. Although the absence of the microfossils is evident in the last part of the section (units 3 and 4), according to the geological position, the lithological and sedimentological characteristics suggest that these strata belong to the lower part of the Svileuva (Werfen) Formation of the lower levels of the Lower Triassic (Fig. 3).

The boundary between the Upper Permian and the Lower Triassic in the investigated section is placed at the level of 9.42 m above the sample KM11. This boundary is a lithological boundary with the evident change of lithological characteristics of the exposed sediments. The sample KM11 could also represent the level of local (?mass) extinction of foraminifers in the section, and for this reason could have biostratigraphic meaning. It is also possible that the absence of foraminifers above the sample KM11 could be also connected with the change of lithofacies.

Conodonts and accompanied isolated microfauna

Conodont dating

A very poor conodont fauna was obtained from the Sitarička Glavica section (samples KM4D, KM4F, KM4G). Preservation of conodont elements is moderate and they are black in color and have a Conodont Alteration Index (CAI) value of approximately 5 *sensu* Epstein et al. (1977). All extracted conodont elements are assigned to the single genus *Hindeodus* of which only the species *Hindeodus praeparvus* Kozur and *H. latidentatus* (Kozur, Mostler & Rahimi-Yazd) are confidently determined. The state of conodont preservation enabled the determination of P1 elements only, because the accompanied ramiform elements are very fragmented. A few of the hindeodid specimens differ from other elements in having a widely open and deeply excavated basal cavity in the central part of the unit and thus show certain similarities with *H. eurypyge* Nicoll, Metcalfe & Wang. Two specimens currently assigned to *Hindeodus* sp. (*H*. ex gr. *H. eurypyge* Nicoll, Metcalfe and Wang) are illustrated in the Fig. 4: 7–8. *H. praeparvus* and *H. eurypyge* first appear in the Changhsingian (Permian) and range also into the lowermost Induan (Triassic). *H. praeparvus* is a widespread zone marker of the last Permian conodont Zone. Based on the absence of *H. parvus*, the collected conodont assemblage is assigned to the *H. praeparvus* Zone. This age is confirmed also by the presence of associated typical Permian, Changhsingian smaller foraminifers and rare fusulinids. The *H. praeparvus* Zone is present in the middle part (samples KM4D–KM4G) of the "Bituminous limestone" (Bellerophon) Formation (Upper Permian, Changhsingian) (Fig. 3).

The investigated isolated microfaunas yield also Late Permian foraminifers present in 11 samples out of 19 (from KM1 to KM11) (Fig. 3). Ostracodes are found in the samples KM2, KM4D, KM4E, KM8 as well as some recrystalized crinoid ossicles in the samples KM4B–KM4E. Moreover, very rare fish teeth are present in the samples KM4A and KM4C.

Comparison of conodont fauna with adjacent areas

The extracted conodont fauna of the Sitarička Glavica section belongs to the *Hindeodus-Isarcicella* lineage and it is assigned to the Changhsingian *Hindeodus praeparvus* Zone. Its presence enables a comparison with coeval conodont faunas of adjacent areas, as well as to faunas from some other important sections of the Palaeotethys (Kozur 2003; Jiang et al. 2007; Farabegoli & Perri 2012; Ogg 2012; Kolar-Jurkovšek & Jurkovšek 2015).

The investigated conodont fauna of the study section is very similar to the conodont fauna from the Komirić section located also in the Jadar Block in NW Serbia. The fauna of both sections are dominated by the species *H. praeparvus* and accompanied by *H. latidentatus*, but with the absence of *Isarcicella* (Sudar et al. 2007).

The species *H. praeparvus* has been so far reported from all sections of the PTB interval that have been studied in the Outer Dinarides as part of the Alpine–Mediterranean belt on the Balkan Peninsula. It is a very common and characteristic species that occurs in the uppermost strata of the Bellerophon Formation (Late Permian, latest Changhsingian) of western Slovenia (Kolar-Jurkovšek et al. 2011a,b; Kolar-Jurkovšek & Jurkovšek 2015).

The Lukač section near Žiri in Slovenia represents a key section to define the PTB interval strata in the Outer Dinarides due to the presence of the conodont species *H. parvus* which is used as a marker of the Permian–Triassic (PT) boundary at the GSSP in Meishan, China (Chen et al. 2015), according to an international criterion of the IUGS (Kolar-Jurkovšek & Jurkovšek 2007). Therefore it is taken also as a standard

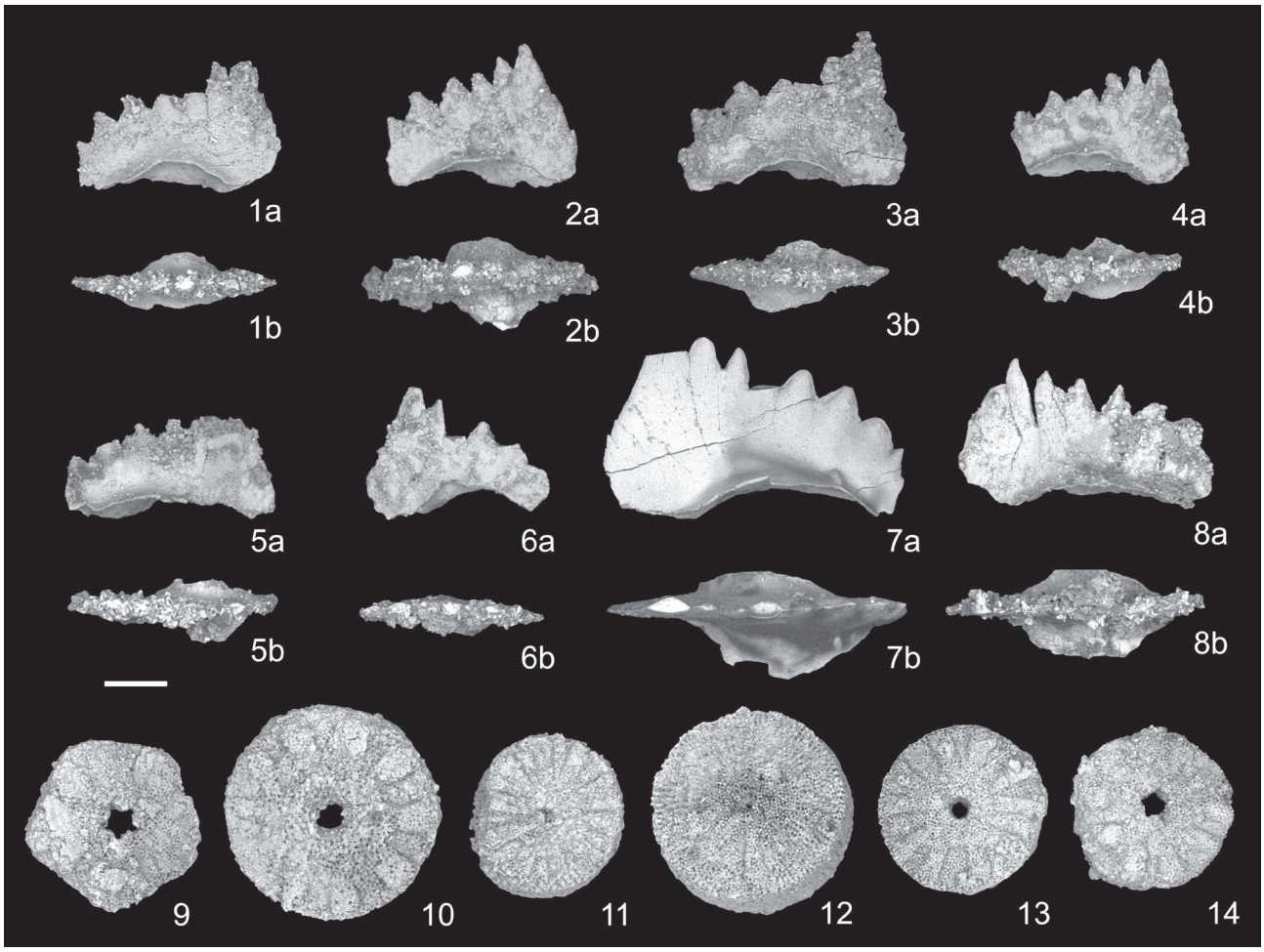

Fig. 4. Conodonts and crinoids from the Upper Permian, Changhsingian, *H. praeparvus* Zone; "Bituminous limestone" (Bellerophon) Formation; Sitarička Glavica section, Jadar Block, NW Serbia. **1, 2, 4** — *Hindeodus praeparvus* Kozur. 1,2 — sample KM4F, 4 — sample KM4G; **3** — *Hindeodus latidentatus* (Kozur, Mostler & Rahimi-Yazd). sample KM4F; **5**, **6** — *Hindeodus* sp. sample KM4E; **7, 8** — *Hindeodus* sp. (*H*. ex gr. *H. eurypyge* Nicoll, Metcalfe & Wang). 7 — sample KM4E, 8 — sample KM4D; **9**–**14** — crinoid ossicles, sample KM4F. a — upper, b — lateral view. Scale bar 100 μm (for Figs. 1–8), and 200 μm (for Figs. 9–14).

section for the conodont zonation for the entire Dinarides area (Kolar-Jurkovšek et al. 2011a, b; 2012; 2013). The association composition of the latest Changhsingian *H. praeparvus* Zone in the Lukač section includes *H. latidentatus, H. praeparvus, H.* cf. *H. pisai*, and *Hindeodus* sp.

Species *H. eurypyge* has been so far documented to occur also in the Outer Dinarides. Its discovery is reported from the Masore section, Slovenia where it appears in association together with the zone markers *H. praeparvus* and *Isarcicella* cf. *I. prisca* (Kolar-Jurkovšek et al. 2018). Moreover, specimens referred to *H.* cf. *H. eurypyge* were collected in the *Isarcicella lobata* Zone of the Lukač section (Kolar-Jurkovšek et al. 2011a, b).

Foraminifers

In the Sitarička Glavica section, the assemblage of foraminifers is represented by species typical for the Upper Permian, Changhsingian (Figs. 5, 6). The assemblage is not diverse and includes 21 species of 15 genera of small foraminifers and four taxa of three genera of fusulinaceans.

Among small foraminifers the dominant forms are hemigordiopsids with a large number of individuals of some genera such as *Hemigordius* and *Neodiscus*. Most tests of these genera are recrystallized and replaced by silica. Besides hemigordiopsids rare nodosariids and globivalvulinids are also present.

The hemigordiopsids are represented by nine species such as *Hemigordius latispiralis* Lin, Li & Sun, *H. komiricensis* Nestell, Sudar, Jovanović & Kolar-Jurkovšek, *H. hungaricus* Bérczi-Makk, Csontos & Pelikán, *Multidiscus vlasicensis* Nestell, Sudar, Jovanović & Kolar-Jurkovšek, *Midiella* sp., *Neodiscus* sp., *Agathammina* cf. *A. psebaensis* Pronina-Nestell, *A.* cf. *A. ovata* Wang, and *A.* sp. 1 (Fig. 3). The presence of recrystallized hemigordiopsids indicates a very shallow environment.

Nodosariids are represented by rare tests of species such as *Protonodosaria mirabilis caucasica* (K. Miklukho-Maklay),

Fig. 5. Foraminifers from the Upper Permian, Changhsingian; "Bituminous limestone" (Bellerophon) Formation; Sitarička Glavica section, Jadar Block, NW Serbia. **1**–**8** — "*Eotuberitina reitlingerae*" Miklukho-Maklay, axial sections. 1, 3 — sample KM2, thin section 71576; 2, 5, 8 — sample KM4, thin section 71614; 4 — sample KM2, thin section 71611; 6, 7 — sample KM4B, thin section 71876; **9**–**11** — *Hemigordius komiricensis* Nestell, Sudar, Jovanović & Kolar-Jurkovšek. 9 — axial section of a completely recrystallized specimen, 10 — close to axial section, 11 — axial section of a partly recrystallized specimen. 9 — sample KM1, thin section 71562; 11 — sample KM4A, thin section 71873; **12**–**16** — *Hemigordius latispiralis* Lin, Li & Sun. 12, 13, 16 — axial sections, 14, 15 — axial sections of completely recrystallized specimens. 12 — sample KM4, thin section 71614; 13 — sample KM4F, thin section 71877; 14 — sample KM11, thin section 71565; 15 — sample KM1, thin section 71562; 16 — sample KM4G, thin section 71832; **17**–**21** — *Hemigordius hungaricus* Bérczi-Makk, Csontos & Pelikán. 17, 18 — close to axial sections, 19, 20, 21 — axial sections of completely recrystallized specimens. 17 — sample KM4F, thin section 71880; 18 — sample KM4, thin section 71568; 19, 20 — sample KM10, thin section 71560; 21 — sample KM11, thin section 71565; **22** — *Midiella* sp., axial section, sample KM4, thin section 71614; **23** — *Agathammina* cf. *A. ovata* Wang, close to axial section, sample KM4A, thin section 71833; **24, 25** — *Multidiscus vlasicensis* Nestell, Sudar, Jovanović & Kolar-Jurkovšek. 24 — axial section, 25 — transverse section; sample KM4E, thin section 71879; **26** — *Neodiscus* sp. 1, close to axial section, sample KM4B, thin section 71876; **27** — *Neodiscus* sp. 2, close to axial section, sample KM4B, thin section 71836. Scale bar 100 μm.

P. delicata (Wang), *Pseudolangella conica* (K. Miklukho-Maklay), *Cryptomorphina limonitica* Sellier de Civrieux & Dessauvagie, *Frondina* cf. *F. paraconica* (K. Miklukho-Maklay), *Geinitzina* cf. *G. orientalis* K. Miklukho-Maklay, *G.* cf. *G. uralica simplex* K. Miklukho-Maklay, *Pachyphloia cukurkoyi* Sellier de Civrieux & Dessauvagie, *Robuloides acutus* Reichel, and *Astacolus permicus* (K. Miklukho-Maklay) (Fig. 3).

Globivalvulinids are represented by single species of the genera *Globivalvulina*, *Retroseptellina*, *Paraglobivalvulina*, and very rare tests of the genus *Dagmarita* (Fig. 3).

All of the listed species of small foraminifers occur in the Changhsingian strata of different regions of the Palaeotethys: in northwestern Serbia (Nestell et al. 2009), western Slovenia (Nestell et al. 2011), in northern Hungary (Bérczi-Makk et al. 1995), northern Italy (Groves et al. 2007), northwestern Caucasus (Miklukho-Maklay 1954; Pronina-Nestell & Nestell 2001), Turkey (Sellier de Civrieux & Dessauvagie 1965; Groves et al. 2005), Transcaucasia (Pronina 1989), and South China (Wang 1976; Zhao et al. 1981; Lin et al. 1990; Zhang & Hong 2004; Song et al. 2006, 2007, 2009).

It should be noted that the attached tests of the unilocular species identified as "*Eotuberitina reitlingerae*" Miklukho-Maklay, are present in almost each sample (from KM1 to KM11). These tests are characterized by varying shapes of the test from bulbous with very narrow basal disk of the attachment (Fig. 5: 2) to crescentiform with a transition from a middle rounded to a wide flattened basal disk of the attachment (Fig. 5: 1, 3–8). Specimens usually consist of one single chamber, but sometimes two chambers can be seen (Fig. 5: 5, 8). In one-chambered tests the wall is microgranular, nonperforate and thin (a characteristic feature for the genus *Eotuberitina* Miklukho-Maklay), whereas in two-chambered forms of the same shape of the chamber the wall is perforate microgranular that, according to definition, is a characteristic feature for the unilocular genus *Tuberitina* Galloway & Harlton. The difference in the wall structure could depend on the maturity of the tests: young specimens have a thin nonperforate wall, whereas older tests have a thicker and perforate wall. Also, the shape of the test could depend on substrates of attachment. Nestell & Nestell (2006, p. 6) showed that in thin sections of their new species *Tuberitina variabilis* from the Middle Permian of West Texas, the shape of the chambers, wall structure and its thickness can vary in one pseudocolony "depending on the position of the section with respect to the center of the test". Based on these statements, the unilocular forms from the Sitarička Glavica section are identified as "*Eotuberitina reitlingerae*" because they have a crescentiform chamber shape like *E. reitlingerae*, although this species is described from the Middle Carboniferous of the Russian Platform (Reitlinger 1950; Miklukho-Maklay 1958). Foraminifers similar to the illustrated herein tests of the species "*Eotuberitina reitlingerae*" are recorded in almost all of the Permian–Triassic transition interval sections studied in the Palaeotethys area, but have been identified by various authors as different genera and species. For example, in the Meishan GSSP section, one-chambered tests with the same shape of the chambers are identified as *Tuberitina* sp. and *Diplosphaerina inaequalis* Derville by Song et al. (2007), or *Eotuberitina reitlingerae* and *Eotuberitina sphaera* Lin by Song et al. (2006). Two-chambered tests were identified by Song et al. (2006) as *Neotuberitina maljavkini* (Mikhailov). In the Dajiang section of the Nanpanjiang basin, both one- and two-chambered tests are identified as the species *Diplosphaerina inaequalis* (Song et al. 2009). In northern Italy, in the Bulla section, one-chambered crescentiform forms are identified as *Diplosphaerina inaequalis* (Groves et al. 2007); in northwestern Serbia, in the Komirić section (Nestell et al. 2009) and in western Slovenia, in the Lukač section (Nestell et al. 2011) — as *Tuberitina*? sp. All of these unilocular forms from the Permian–Triassic transition interval are probably the same, and possibly represent a new species which could be described after a careful revision of all unilocular forms of the family Tuberitinidae with a precise definition of each genus and its stratigraphic distribution.

Fusulinaceans are very rare and represented by only three species such as *Staffella* cf. *S. hupehensis* Jing, *Nankinella* cf. *N. chongyangensis* Jing, and *Nankinella* cf. *N. acuta* Lin in the sample KM4D. Representatives of the genus *Palaeofusulina* are extremely rare; only two tangential sections were seen which did not allow identification on the specific level. The species *Staffella hupehensis* and *Nankinella chongyangensis* have been described from Changhsingian strata in southern part of the Hubei Province (Jing 1992) and the species *Nankinella acuta* from western Guizhou Province, China (Lin 1979).

The distribution of foraminiferal species in the Sitarička Glavica section is given in Fig. 3. The only occurrence of fusulinacean species are in sample KM4 (KM4A, KM4D). Among abundant presence of small foraminifers in the lower part of the Sitarička Glavica section, only four species of these microfossils continue into sample KM11 (Fig. 3: A). No foraminifers were found in sample KM12 and above, in the upper part of the section.

Usually, in Permian–Triassic boundary interval sections described from many places of the world, the diverse latest Permian assemblage of foraminifers is replaced by small tests of opportunistic species of the genera *Hyperammina* (former *Earlandia*) and *Ammodiscus* (former *Cornuspira* or *Postcladella*) together with microconchids (Brönnimann et al. 1972; Bérczi-Makk 1987; Groves et al. 2005, 2007; Song et al. 2009; Nestell et al. 2011, 2015), an association that is not seen in the Sitarička Glavica section.

We cannot say for sure that sample KM11 represents the level of mass extinction of foraminifers in the section, and their absence above this sample could possibly be connected with changing lithofacies. However, the distribution and extinction sequence of the genera of foraminifers (Fig. 3: B), and their last appearance, in general, coincides with the distribution and extinction of the genera observed at the Permian–Triassic boundary interval in the Lung Cam section of northern Vietnam (Nestell et al. 2015). In both sections, Sitarička Glavica and Lung Cam, the mass extinction of foraminifers

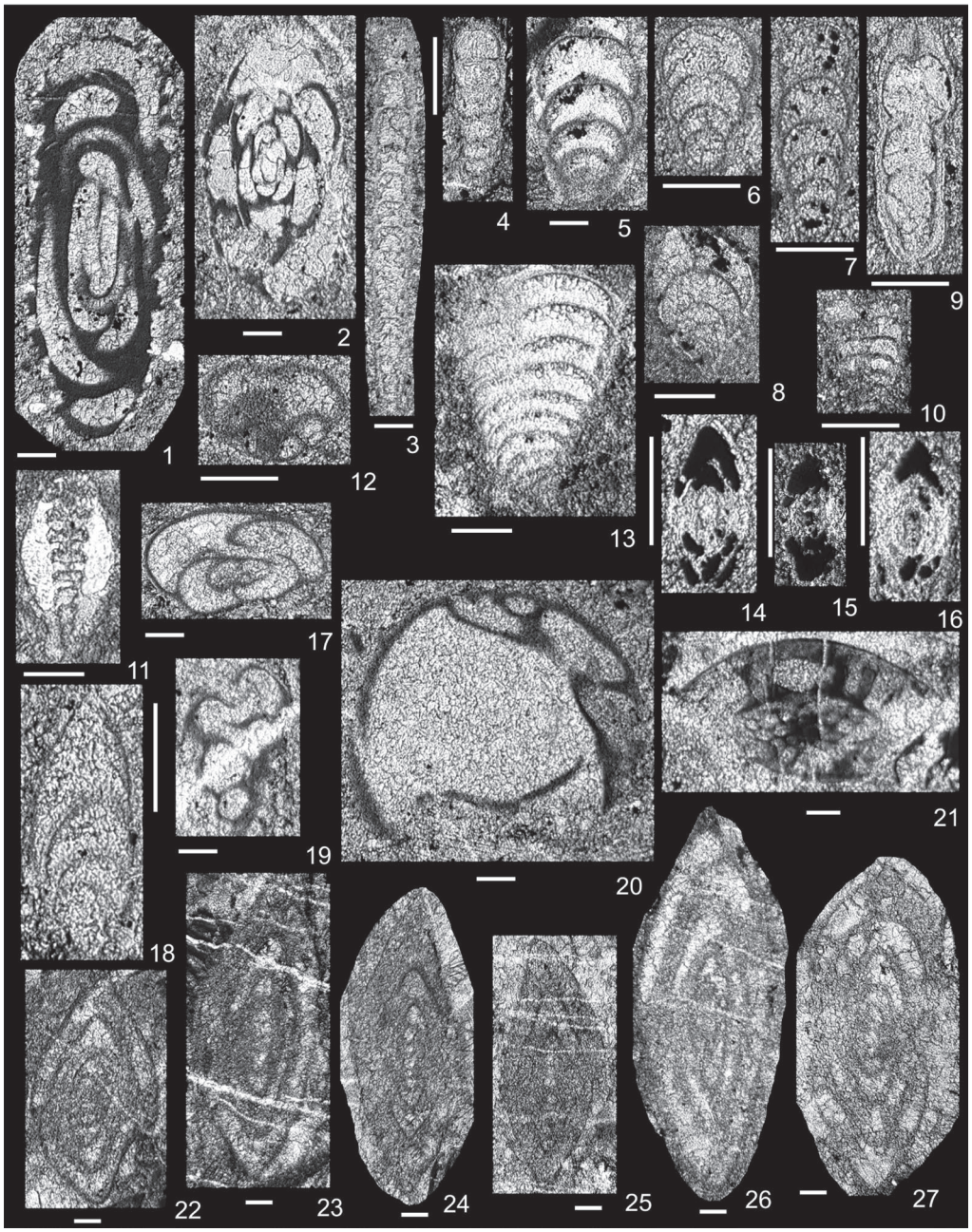

Fig. 6. Foraminifers from the Upper Permian, Changhsingian; "Bituminous limestone" (Bellerophon) Formation; Sitarička Glavica section, Jadar Block, NW Serbia. **1** — *Agathammina* cf. *A. psebaensis* Pronina-Nestell, close to axial section, sample KM4, thin section 71614; **2** — *Agathammina* sp. 1, axial? section, sample KM2, thin section 71611; **3** — *Protonodosaria mirabilis caucasica* (K. Miklukho-Maklay), close to axial section, sample KM4B, thin section 71876; **4** — *Protonodosaria delicata* (Wang), close to axial section, sample KM4G, thin section 71832; **5** — *Pseudolangella conica* (K. Miklukho-Maklay), close to axial section, sample KM4, thin section 71614; **6, 7** — *Frondina* cf. *F. paraconica* (K. Miklukho-Maklay). 6 — axial tangential section, sample KM2, thin section 71613; 7 — lateral section, sample KM4B, thin section 71876; **8** — *Frondina* sp. 1, axial tangential section, sample KM9, thin section 71559; **9** — *Cryptomorphina limonitica* Sellier de Civrieux & Dessauvagie, axial section, sample KM4F, thin section 71880; **10** — *Geinitzina* cf. *G. orientalis* K. Miklukho-Maklay, close to axial section, sample KM2, thin section 71576; **11** — *Pachyphloia cukurkoyi* Sellier de Civrieux & Dessauvagie, axial lateral section, sample KM7, thin section 71573; **12** — *Globivalvulina lukachiensis* Nestell, Kolar-Jurkovšek, Jurkovšek & Aljinović, tangential section, sample KM4B, thin section, 71836; **13** — *Geinitzina* cf. *G. uralica simplex* K. Miklukho-Maklay, axial tangential section, sample KM2, thin section 71613; **14**–**16** — *Robuloides acutus* Reichel, axial sections. 14 — sample KM4F, thin section 71877; 15 — sample KM2, thin section 71613; 16 — sample KM4C, thin section 71878; **17** — ?*Retroseptellina nitida* (Lin, Li & Sun), tangential section, sample KM6, thin section 71561; **18** — *Astacolus permicus* (K. Miklukho-Maklay), close to axial section, sample KM4B, thin section 71836; **19** — *Dagmarita* sp., axial tangential section, sample KM4B, thin section 71836; **20** — *Paraglobivalvulina* cf. *P. gracilis* Zaninetti & Altiner, tangential section, sample KM4, thin section 71614; **21** — ?*Palaeofusulina* sp., tangential section, sample KM4A, thin section 71873; **22** – *Nankinella* cf. *N. chongyangensis* Jing, close to axial section, sample KM4, thin section 71568; **23**–**26** — *Nankinella* cf. *N. acuta* Lin, axial sections. 23 — sample KM4, thin section 71568; 24, 25, 26 — sample KM4, thin section 71614; **27** — *Staffella* cf. *S. hupehensis* Jing, axial section, sample KM4, thin section 71615. Scale bar 100 μm.

happens step by step. The difference in the distribution of genera of foraminifers between two sections is in the survival of the genera *Globivalvulina*, *Geinitzina* and *Nodosaria* after the mass extinction in the Lung Cam section, whereas in the Sitarička Glavica section these genera are extinct in sample KM11, which is, most probably, the level of mass extinction in this section. The first appearance of the microconchid genus *Microconchus* is in sample KM16. The genus appears in the latest Permian and continues into the early Triassic (Brönnimann & Zaninetti 1972; Nestell et al. 2015).

Geochemical investigations

Brookfield and Williams (in 2011), Brookfield (in 2013) together with Sudar and Jovanović measured in detail the Sitarička Glavica section and took samples for the geochemical and sedimentological investigations, with preliminary results reported in Williams et al. (2013a,b; 2014). Although the detailed elemental and isotope geochemistry will be given elsewhere, herein we summarize some of the main results and suggest some causes.

Four negative $\delta^{13}C_{org}$ excursions are recorded in this PTB section (Fig. 7A). Excursion #1 (−3 m to −0.5 m, ~−7 ‰), excursion #2 (−0.05 m to 2 m, ~−1.6 ‰), excursion #3 (3 m to 4 m, ~−4.3 ‰), and excursion #4 (5 m to 8 m, ~−2.5 ‰). The four negative $\delta^{13}C_{org}$ excursions are associated with changes in lithofacies from gray to dark shale (excursion #1), and changes in fauna (excursions 2–4). The 2nd and 3rd excursion straddle the PTB, the 2nd excursion with the appearance of crinoids, brachiopods, bryozoan, foraminifers, and molluscs, whereas the 3rd excursion occurs with only molluscs.

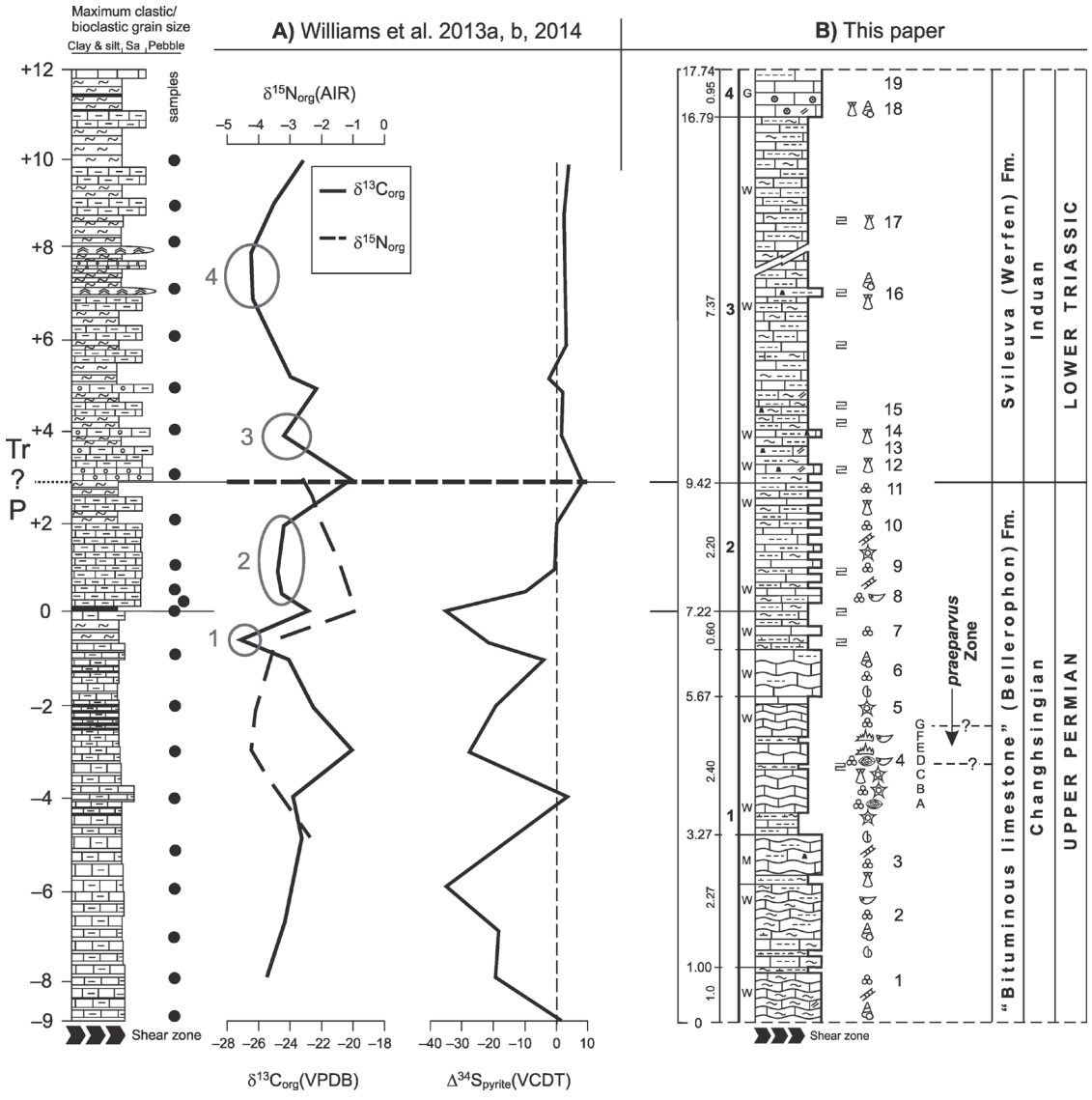

Fig. 7. Parallel review of the results of geochemical (Willams et al. 2013a,b; 2014: **7A**) and stratigraphic/biostratigraphic investigations (this paper: **7B**) in the Sitarička Glavica section, Jadar Block, NW Serbia. The four negative $\delta^{13}C_{org}$ excursions recorded in the section are shown on Fig. **7A**.

The 4th excursion, occurs with the stromatolite-like bed (Fig. 7A and KM16 of Unit 3 in Fig. 7B). These negative shifts are indicative of a decrease in primary productivity. The abrupt decrease $\delta^{13}C_{org}$ suggest a crash in the biological pump (Kump 2005), creating a biological crisis. Excursion #1 and #2 are similar to the $\delta^{13}C_{org}$ signature of the GSSP Meishan section, which occurs before the PTB (Korte & Kozur 2010). Like other PT sections in the Palaeotethys, Sitarička Glavica $\delta^{13}C_{org}$ signature suggests a major perturbation in the C-cycle during the extinction interval and a long recovery.

The $\delta^{15}N_{org}$ signature suggests that the surface waters were dominated by N-fixation, derived from diazotrophs that converted atmospheric N into NH_4 (Fig. 7A; Quan & Falkowski 2009). The depleted signature may suggest low depositional oxygen conditions. The negative excursion recorded near the PTB is similar to Rizvanuša, Croatia (Fio et al. 2010), Guryul Ravine, Kashmir, India (Algeo et al. 2007) and GSSP Meishan, South China (Cao et al. 2009; Luo et al. 2011). This abrupt negative shift maybe attributed to catastrophic conditions where the ecological disaster resulted in enhancement of N-fixation from widespread diazotrophs (Luo et al. 2011).

The $\delta^{34}S_{pyrite}$ signature suggests decoupling of the S-cycle during the Late Permian due to the fluctuations from enriched to depleted $\delta^{34}S_{pyrite}$ (Fig. 7A). Framboidal pyrite occurs in the Bellerophon Formation, whereas oxidized pyrite is present in the Werfen Formation. Framboids occur between −9 m to 3 m (PTB) suggesting syngenetic formation (Fig. 8; Williams 2013b). The depleted $\delta^{34}S_{pyrite}$ signature along with the presence of framboidal pyrite strongly suggests widespread oxygen depletion (Shen et al. 2007). Evidence of framboids coupled with positive $\delta^{34}S_{pyrite}$ values (−9 m, −4 m, and 3 m) suggest a closed S-system where the SO_4^{2-} reduction exceeds the supply, with the ensuing Rayleigh fractionation causing an enriched isotopic signal (Figs. 7A, 8; Williford et al. 2009). Oxidizing framboids occur between 4 m to 10 m, indicating late diagenetic formation. The occurrence of partially oxidized framboids (5 m) is indicative of syngenetic and late diagenetic formation (Figs. 7A, 8; Williams et al. 2013b). At the PTB, evidence of both framboidal and euhedral pyrite suggest both syngenetic and precipitation formation. Euhedral formation through precipitation formation is probably due to the occurrence of an oolite factory at the PTB from the decrease in skeletal CO_3^{2-} (Haas et al. 2007; Li et al. 2015). The presence of oolite and euhedral pyrite along with a coral gap, may serve as evidence of widespread ocean acidification in the Palaeotethys during the extinction interval (Li et al. 2015).

The elemental geochemical changes across the PTB in the Sitarička Glavica section are minimal, which indicates little physical environmental change, such as source type and conditions. We plot element/Al ratios to identify anomalies due to biology or geochemistry, which show up as deviations from average element/Al values and values of reference sediments (Calvert & Pedersen 1993). The ratios are shown on arithmetic log plots to emphasize the order of magnitude differences as the actual values are frequently so low as to make small differences appear important on arithmetic plots. For the major elements, Si/Al, Ti/Al, Fe/Al and Mn/Al ratios change little through the section, showing that these elements correlate with Al (Fig. 9). Mg/Al, Ca/Al and K/Al tend to drop above the extinction horizon, whereas Na/Al tends to rise as the lithologies change to less carbonate-dominated. For the minor elements, the ratios to Al change little except for high values of most ratios within 1 meter of the Bellerophon/Werfen contact, in beds 8 to 11 during the $\delta^{13}C_{org}$ and $\delta^{15}N_{org}$ and $\delta^{34}S_{pyrite}$ positive excursions; above which Sc/Al, Ge/Al, Zr/Al, Nb/Al, Hf/Al, Th/Al tend to increase, whereas Be/Al, B/Al, Ni/Al,

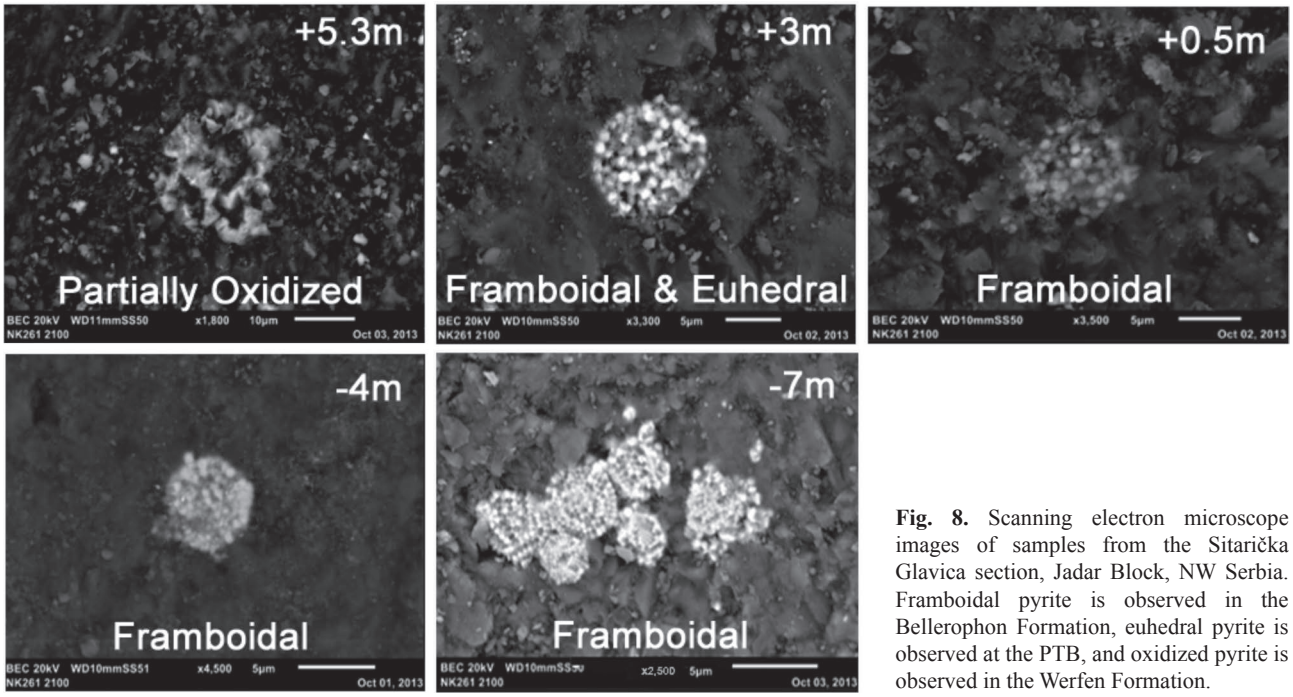

Fig. 8. Scanning electron microscope images of samples from the Sitarička Glavica section, Jadar Block, NW Serbia. Framboidal pyrite is observed in the Bellerophon Formation, euhedral pyrite is observed at the PTB, and oxidized pyrite is observed in the Werfen Formation.

As/Al, Y/Al, Mo/Al, Sn/Al, Sb/Al, Cs/Al, Pb/Al, and U/Al tend to drop, and TOC/Al drops by an order of magnitude (Williams et al. 2014).

The source character can be inferred from various indices. The Chemical Index of Alteration (CIA) summarizes chemical alteration during weathering, transportation and deposition and gives geochemical estimations of provenance (Nesbitt & Young 1982). The Index of Compositional Variability (ICV) includes Fe, Mg, and Mn, and does not require calculation of non-carbonate Ca, and uses oxides rather than moles (Cox et al. 1995). Average basalt and average granite have very different ICV values of 2.20 and 0.95 (Li 2000). So, mudstone with the same degree of weathering (the same CIA) may have different ICV values, indicating composition of the source area; though calcareous sediments give misleading values in all cases. The calcareous Serbian sediments (minimum CaO is 12.77 %) are all misleading as their ICV values are at or higher than the basalt value. But, Serbian CIA values for samples with less than 50 % of carbonate are 56–72, and indicate a moderate degree of chemical weathering of the parent material with no marked changes up the section, and are comparable to reference sandy and silty mudstone, and to Recent North American and Asian rivers (Li & Yang 2010) (Fig. 10).

The Na/K, K/Fe, and K/Fe+Mg ratios can similarly be used to infer source characteristics and weathering. Na/K ratios reflect the maturity of clastic sediments. Na/K ratios above 1 indicate immature sediments, whereas those below 1 indicate more mature sediments. The Serbian sediments have generally more mature Na/K ratios below the extinction horizon in the more calcareous beds and less mature (but still below 1) above (Fig. 10).

K/Fe and K/(Fe+Mg) ratios reflect the contribution of acidic versus basic rocks and the rate of chemical weathering of K-felspar (Nesbitt et al. 1997). In areas of diverse rock sources like the present Atlantic margins, relatively low K/Fe values of tropical areas (0.26) contrast with higher K/Fe values (0.43) for arid regions (Govin et al. 2012). Serbian K/Fe values are all higher than the arid region values except for two at +2 m and +3 m straddling the extinction level. This range of values is not only compatible with the extreme aridity inferred for Permian–Triassic (PTr) source areas in the PTr palaeotropics (Brookfield 2008), but with the possible wetter pluvial interval at the PT boundary in northern Gondwanaland (Kreuser 1995). The values above 0.5 probably indicate volcanic input (Sageman & Lyons 2005). The Serbian K/(Fe+Mg) ratios do not change much up section, but have a low at the extinction

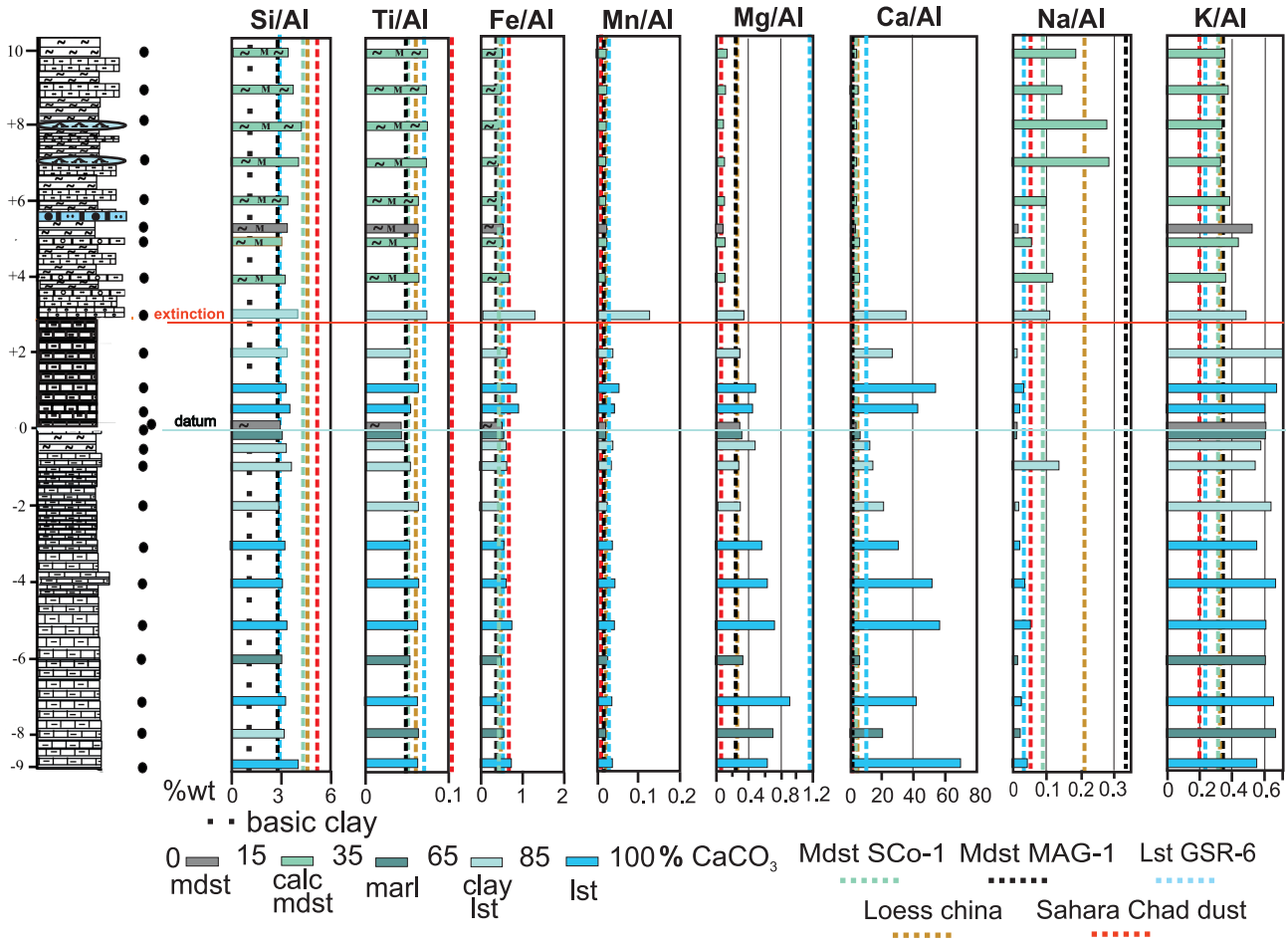

Fig. 9. Majors ratios to Al.

horizon, and are close to clastic reference sediment values, but much higher than the reference limestone (Fig. 10).

In the West African deserts and the adjacent eastern Atlantic, high Ti/Zr values occur in dust aerosols and marine clays supplied from dust aerosols (>38–40) where softer abraded ilmenite dust is concentrated, whereas lower values occur in river and coastal clay sediments which are derived in part from remobilized eolian lags (<30) where abrasion-resistent zircons are concentrated (Govin et al. 2012; Patey et al. 2015). The reference low Ti/Zr Chinese loess and Sahara Chad dust values are misleading because the samples come from Quaternary dust adjacent to and derived from bedrock sources only locally remobilized by wind — particles have not had time to significantly abrade. Only two Serbian Ti/Zr values (at −8 m and +0.05 m) reach anywhere near eolian values, and thus most of the Serbian clays come from fluvial sources (Fig. 10).

Nb/Ta ratios decrease in clays from arid areas (Nb/Ta ~15) to humid areas (Nb/Ta ~8.5), as Nb is preferentially leached. Serbian Nb/Ta ratios vary little around the remarkably constant reference sediment value of 10, and are only slightly less than the average Upper Continental Crust values of 13 (Barth et al. 2000), though there is a tendency to have slightly lower values around the PT boundary which may reflect wetter conditions (Fig. 10).

Climatic change in source regions, without source composition changes, can be determined by fluctuations in Ti/Al, Ti/K and Ti/Sc ratios. Wei et al. (2003) showed that sharp changes in these correlated with Quaternary glacial/interglacial cycles, with higher ratios in warmer periods due to increased chemical weathering. In eastern Atlantic surface sediments off the West African deserts, intermediate Ti/Al values in areas of high dust deposition contrast with Ti/Al values in areas dominated by the input of suspended material from the Senegal, Niger and Congo rivers (Govin et al. 2012). Serbian Ti/Al ratios show little change except for a slight drop in unit 2 (the last 2.20 meters of the "Bituminous limestone" (Bellerophon) Formation) and slight increase above (Fig. 10).

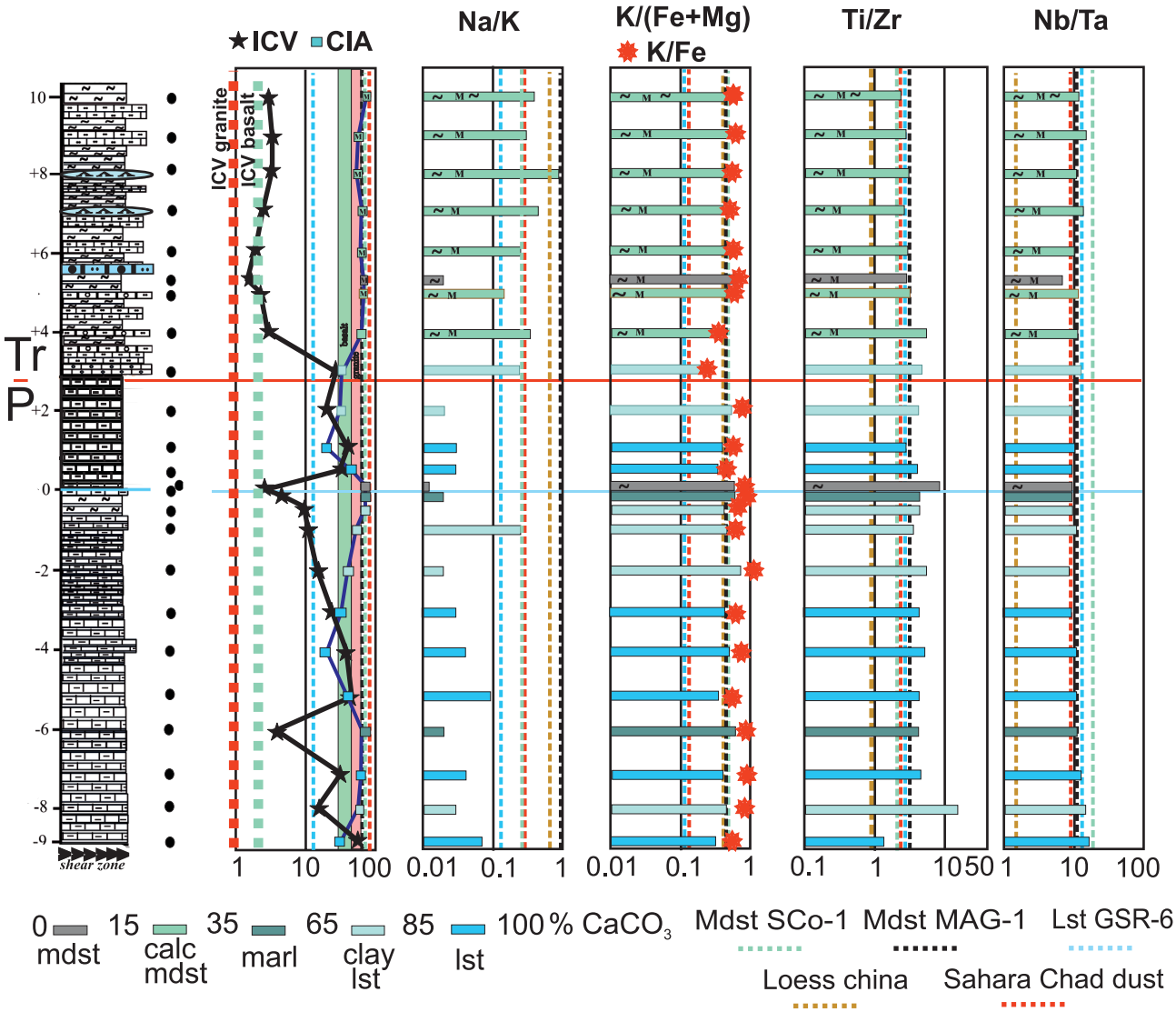

Fig. 10. CIA, ICV, Na/K, K/(Fe+Mg), Ti/Zr, Nb/Ta ratios.

Various redox proxies involving transition elements and U are commonly used such as V/Cr, V/(V+Ni), Ni/Co, U/Mo and U/Th and though they are unreliable individually together, they give better results (Wignall & Myers 1988; Jones & Manning 1994; Tribovillard et al. 2006; Zhou et al. 2012). Serbian V/Cr are all in the oxic field: V (V+Ni) are in the oxic field in Unit 1 and are in the dysoxic field around 0 m and above +4 m; Ni/Co are in the suboxic-anoxic field below −1 m and are in the dysoxic and oxic fields above, with some reversals to suboxic-anoxic; U/Mo are mostly in the suboxic-anoxic fields; Th/U are mostly in the subxic-anoxic field until +4 m above which they are predominantly oxic (Fig. 11). There is thus no consistency in these redox proxies in the Serbian sediments; though on Ni/Co, U/Mo, Th/U conditions were dysoxic below +4 m and oxic above +4 m. Th/U ratios give more dysoxic conditions than the Mo/Al ratios though they follow the same trends. The lack of consistency in these redox proxies is disappointing, but anoxia seems present in units 1 and 2 with oxic conditions in Unit 3 above (Fig. 11).

Conclusions

The detail palaeontological, sedimentological and geochemical investigations of strata from the PTB interval in Sitarička Glavica section (Jadar Block, Valjevo, NW Serbia) exhibit various and important features which can be summarized as follows:

- Abundant and diverse macro- and microassociations recorded exclusively in the lower part of the section enabled the determination of the Changhsingian Stage within the Upper Permian "Bituminous limestone" (Bellerophon) Formation. The investigated conodont fauna from the middle part of the Permian part of the section belongs to the *Hindeodus-Isarcicella* lineage and, according to their biostratigraphic characteristics, it is assigned to the Changhsingian *Hindeodus praeparvus* Zone. The assemblage of foraminifers is richer, represented by species typical for the Upper Permian, Changhsingian, in the lower part of the section.

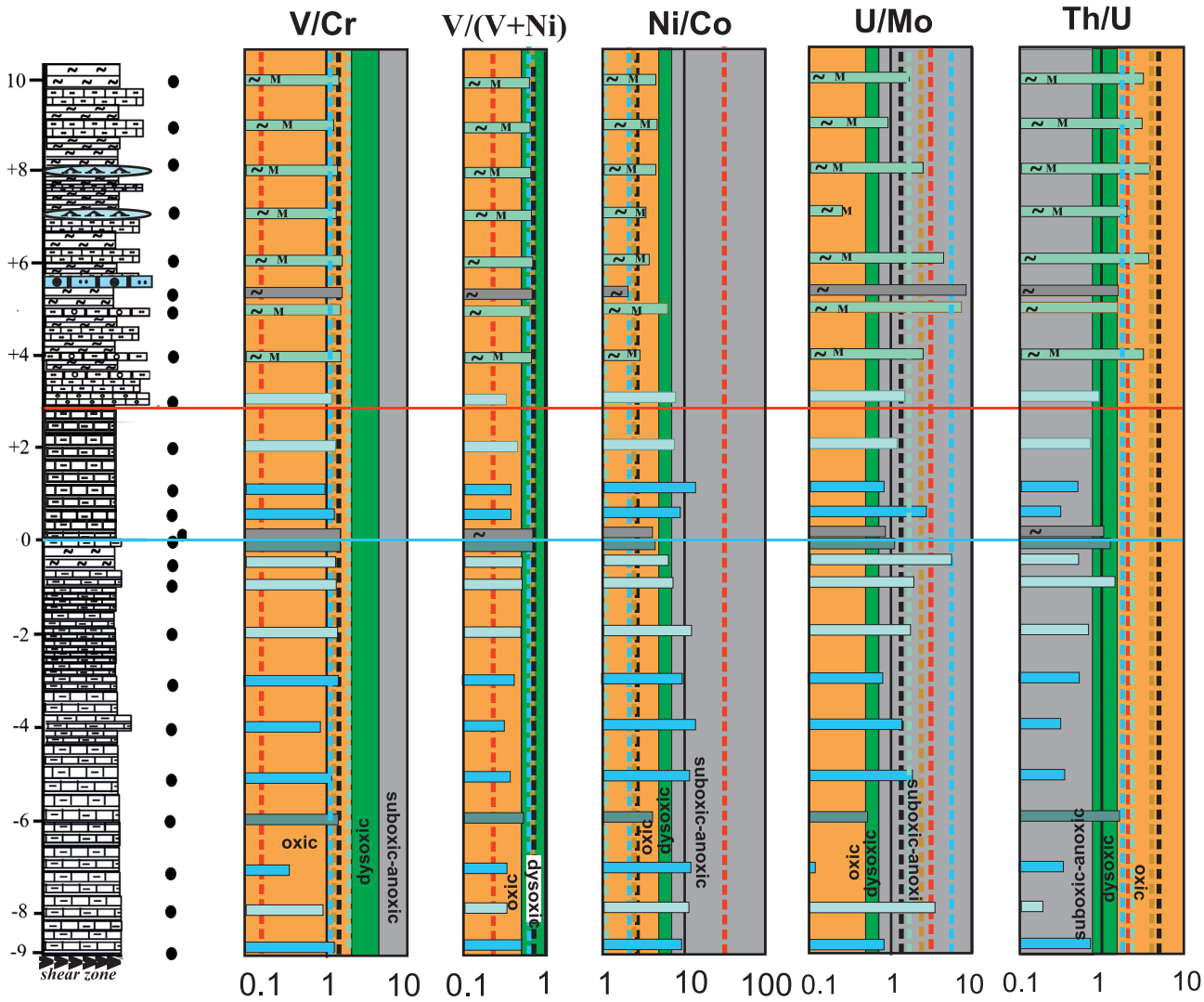

Fig. 11. V/Cr, V(V+Ni), Ni/Co, U/Mo, Th/U.

- The second part of the section (units 3 and 4) is without microfossils (only rare sections and fragments of molluscs), with clearly a change of sedimentologic characteristics and geological/superpositional position determinated as Lower Triassic, i.e. the lower part of the Svileuva (Werfen) Formation.
- The boundary between the Upper Permian and the Lower Triassic is placed at the level of 9.42 m of the section above the sample KM11. This boundary is a lithologic boundary and has also biostratigraphic importance. It is marked by a rapid change of sedimentological characteristics and with the clear absence of microfossils in the upper part of the exposed sediments. The sample KM11 could also represent the level of local (?mass) extinction of foraminifers in the section, as confirmed by the changing of lithofacies.
- Although in all of the PTB investigated sections in NW Serbia we have not yet found conodonts and foraminfers of the lowermost parts of the Lower Triassic, the presence of their coeval assemblages of the Late Permian, Changhsingian age in Jadar Block of NW Serbia, enables correlation with many regions of the Palaeotethys: e.g., in western Slovenia, northeastern Hungary, northern Italy, northwestern Caucasus, Turkey, Transcaucasia, and South China. The present study can be added to the list of well-known and important localities of the PTB interval; the results may contribute to improve the precision of the Tethys-wide and even worldwide correlation of the boundary events.
- Geochemical investigations undertaken for the first time in the region as well as from all of Serbia, show that stable isotopes (C, N, S), mineralogy, major and trace elements of the studied PTB interval section have similar patterns of secular variation as in other well known marine Upper Permian sections, suggesting major changes in sediment provenance and marine environmental conditions prior to the Lower Triassic, where geochemical proxies indicate prolonged seawater anoxia.
- Geochemical changes of the Sitarička Glavica PTB sediments indicate a moderate degree of chemical weathering of the parent material with no marked changes up the section and an arid to semi-arid climate at the source. The Upper Permian sediments are perhaps slightly more mature, and there is a suggestion of a wetter phase around the PT boundary at the time of large lakes in northern Pangea. Until just above the PT boundary at +4 meters, suboxic conditions seem to have dominated, than conditions became predominantly oxic, but the various redox proxies do not correlate well.

Acknowledgments: We are very grateful to Merlynd K. Nestell (University of Texas at Arlington) for the identifications of fusulinacean species and checking English. Communication and discussion on conodonts with Charles M. Henderson (Calgary, Canada) are acknowledged. The study was partly supported by the Slovenian Research Agency (programme P1-0011). This paper is a contribution to IGCP 630, and to the bilateral project cooperation between Serbian and Slovenian Academies of Sciences and Arts (Project F-12). The research of the authors from Serbia was supported by the Ministry of Education, Science and Technical Development of the Republic of Serbia (Project ON-176015). The critical comments and helpful suggestions of two reviewers, Zhong-Quing Chen (Wuhan, China) and Ian Metcalfe (Armidale, Australia), helped to improve the quality of the paper and are gratefully acknowledged.

References

Algeo T.J., Hannigan R., Rowe H., Brookfield M., Baud A., Krystyn L. & Ellwood B.B. 2007: Sequencing events across the Permian–Triassic boundary, Guryul Ravine (Kashmir, India*). Palaeogeogr. Palaeoclimatol. Palaeoecol.* 252, 1, 328–346.

Barth M.G., McDonough W.F. & Rudnick, R.L. 2000: Tracking the budget of Nb and Ta in the continental crust. *Chem. Geol.* 165, 197–215.

Bérczi-Makk A. 1987: *Earlandia* (Foraminifera) species from the Permian–Triassic boundary in N Hungary. *Magyar Állami Földtani Intézet evi Jelentése Az 1985, Évről v*. 1987, 215–226.

Bérczi-Makk A., Csontos L. & Pelikán P. 1995: Data on the (Upper Permian) foraminifer fauna of the Nagyvisnyó Limestone Formation from borehole Mályinka-8 (northern Hungary). *Acta Geol. Hung.* 38, 185–250.

Brönnimann P. & Zaninetti L. 1972: On the occurrence of the serpulid *Spirorbis* Daudin, 1800 (Annelida, Polychaetia, Sedentarida) in thin sections of Triassic rocks of Europe and Iran. *Rivista Italiana et Paleontologica* 78, 67–90.

Brönnimann P., Zaninetti L. & Bozorgnia F. 1972: Triassic (Scythian) smaller foraminifera from the Elika Formation of the central Alborz, northern Iran, and from the Siusi Formation of the Dolomites, northern Italy. *Mitteilungen Der Gessellschaft der Geologie und Bergbaustudenten* 21, 861–884.

Brookfield M.E. 2008: Palaeoenvironments and palaeotectonics of the arid to hyperarid intracontinental latest Permian–late Triassic Solway basin (U.K.). *Sediment. Geol.* 210, 27–47.

Calvert S.E. & Pedersen T. 1993: Geochemistry of recent oxic and anoxic marine sediments: implications for the geological records. *Mar. Geol.* 11, 67–88.

Cao Ch., Love G.D., Hays L.E., Wang W., Shen Sh. & Summons R.E. 2009: Biogeochemical evidence for euxinic oceans and ecological disturbance presaging the end-Permian mass extinction event. *Earth Planet. Sci. Lett.* 281, 3–4, 188–201.

Chen Z.-Q., Yang H., Luo M., Benton M.J., Kaiho K., Zhao L., Huang YG., Zhang K., Fang Y., Jiang H., Qiu H., Li Y., Tu C., Shi L., Zhang L., Feng X. & Chen L., 2015: Complete biotic and sedimentary records of the Permian–Triassic transition from Meishan section, South China: Ecologically assessing mass extinction and its aftermath. *Earth-Sci. Rev.*149, 67–107.

Cox R., Lowe D. R. & Cullers R.L. 1995: The influence of sediment recycling and basement composition of evolution of mudrock chemistry in the southwestern United States. *Geochim. Cosmochim. Acta* 59, 2919–2940.

Crasquin S., Sudar M.N., Jovanović D. & Kolar-Jurkovšek T. 2010: Upper Permian ostracode assemblage from the Jadar Block (Vardar Zone, NW Serbia). *Geološki anali Balkanskoga poluostrva* (Beograd) 71, 23–35 (in English with Serbian summary).

Epstein A.G., Epstein J.B. & Harris L.D. 1977: Conodont Color Alteration — An Index to Organic Metamorphism. *US Geol. Surv. Prof. Pap.* 995, 1–27.

Farabegoli E. & Perri M.C. 2012: Millenial Physical Events and the End-Permian Mass Mortality in the Western Palaeotethys: Timing and Primary Causes. In: Talent J.A. (Ed.): International Year of Planet Earth. *Springer Science+Business Media B.V.*, 719–758.

Filipović I., Jovanović D., Sudar M., Pelikán P., Kovács S., Less Gy. & Hips K. 2003: Comparison of the Variscan-Early Alpine evolution of the Jadar Block (NW Serbia) and "Bükkium" (NE Hungary) terranes; some paleogeographic implications. *Slovak Geol. Mag.* 9, 1, 23–40.

Fio K., Spangenberg J.E., Vlahović I., Sremac J., Velić I. & Mrinjek E. 2010: Stable isotope and trace element stratigraphy across the Permian–Triassic transition: A redefinition of the boundary in the Velebit Mountain, Croatia. *Chem. Geol.* 278, 1, 38–57.

Govin A., Holzwarth U., Heslop D., Keeling L.F., Zabel M., Mulitza S., Collins J.A. & Chiessi C.M. 2012: Distribution of major elements in Atlantic surface sediments (36oN-49oS): imprint of terrigenous input and continental weathering. *Geochem. Geophys. Geosyst.* 13, doi:10.1029/2011GC003785.

Groves J.R., Altiner D. & Rettori R. 2005: Extinction, survival, and recovery of Lagenide foraminifers in the Permian–Triassic boundary interval, central Taurides, Turkey. *J. Paleontology* Memoir 62, Supplement to no. 4, 1–38.

Groves J.R., Rettori R., Payne J.L., Boyce M.D. & Altiner D. 2007: End-Permian mass extinction of lagenide foraminifers in the Southern Alps (northern Italy). *J. Paleontol.* 81, 415–434.

Haas J., Demény A., Hips K., Zajzon N., Weiszburg T.G., Sudar M. & Pálfy J. 2007: Biotic and environmental changes in the Permian–Triassic boundary interval recorded on a western Tethyan ramp in the Bükk Mountains, Hungary. *Global Planet. Change* 55, 1, 136–154.

Jiang H., Lai X., Luo G., Aldridge R., Zhang K. & Wignall P. 2007: Restudy of conodont zonation and evolution across the P/T boundary at Meishan section, Changxing, Zhejiang, China. *Global Planet. Change* 55, 1–3, 39–55.

Jing M. 1992: The Late Permian fusulinids in south Hubei. *Meitian Dizhi Yu Kantan=Coal Geology and Exploration* 20, 15–21 (in Chinese with English abstract).

Jones B. & Manning D.A.C. 1994: Comparison of geochemical indices used for the interpretation of palaoeredox conditions in ancient mudstones. *Chem. Geol.* 111, 111–129.

Karamata S. 2006: The geological development of the Balkan Peninsula related to the approach, collision and compression of Gondwanan and Eurasian units. In: Robertson, A.H.F & Mountrakis, D. (Eds.): Tectonic Development of the Eastern Mediterranean Region. *Geol. Soc. London, Spec. Publ.* 260, 155–178.

Karamata S., Olujić J., Protić Lj., Milovanović D., Vujnović L., Popević A., Memović E., Radovanović Z. & Resimić-Šarić K. 2000: The Western Belt of the Vardar Zone — the remnant of a marginal sea. In: Karamata S. & Janković, S. (Eds.): Proceedings of the International Symposium "Geology and Metallogeny of the Dinarides and the Vardar Zone". *Academy of Sciences and Arts of the Republic of Srpska, Collections and Monographs* I, *Department of Natural, Mathematical and Technical Sciences* I, 131–135.

Kolar-Jurkovšek T. & Jurkovšek B. 2007: First record of *Hindeodus-Isarcicella* population in Lower Triassic of Slovenia. *Palaeogeogr. Palaeoclimatol. Palaeoecol.* 252, 72–81.

Kolar-Jurkovšek T. & Jurkovšek B. 2015: Conodont zonation of Lower Triassic strata in Slovenia. *Geologija* (Ljubljana) 58/2, 155–174.

Kolar-Jurkovšek T., Jurkovšek B. & Aljinović D. 2011a: Conodont biostratigraphy and lithostratigraphy across the Permian–Triassic boundary at Lukač section in western Slovenia. *Rivista Italiana di Paleontologia e Stratigrafia* 117/1, 115–133.

Kolar-Jurkovšek T., Jurkovšek B., Aljinović D. & Nestell G.P. 2011b: Stratigraphy of Upper Permian and Lower Triassic Strata of the Žiri Area (Slovenia). *Geologija* (Ljubljana) 54/2, 193–204.

Kolar-Jurkovšek T., Jurkovšek B., Aljinović D. & Nestell G.P. 2012: Lukač section — a key for a definition of the Permian–Triassic boundary in the Dinarides. In: IGCP 572 Closing Conference, Eger, Hungary. *Abstract volume & field guide — Bükk Mountains,* 21–22.

Kolar-Jurkovšek T., Jurkovšek B., Nestell G.P. & Aljinović D. 2013: Permian - Triassic boundary interval in Slovenia: new micropaleontological data. In: Albanesi G.L. & Ortega G. (Eds.). Conodonts from the Andes: proceedings of the 3rd International Conodont Symposium, *Asociación Paleontológica Argentina,* Buenos Aires, 143.

Kolar-Jurkovšek T., Jurkovšek B., Nestell G.P. & Aljinović D. 2018: Biostratigraphy and Sedimentology of Upper Permian and Lower Triassic Strata at Masore, Western Slovenia. *Palaeogeogr. Palaeoclimatol. Palaeoecol.* 490, 38–54.

Korte C. & Kozur H.W. 2010: Carbon-isotope stratigraphy across the Permian–Triassic boundary: a review. *J. Asian Earth Sci.* 39, 4, 215–235.

Kozur H. 2003: Integrated ammonoid, conodont and radiolarian zonation of the Triassic. *Hallesches Jahrbuch für Geowissenschaften* B 25, 49–79.

Kreuser T. 1995: Tectonic and climatic controls of lacustrine sedimentation in pre-rift and rift settings in the Permian–Triassic of East Africa. *J. Paleolimnology* 13, 3–19.

Kump L.R. 2005: The Geochemistry of Mass Extinction. In: Mackenzie F.T. (Ed.): Sediments, diagenesis and sedimentary rocks. *Treatise on Geochemistry* 7, *Elsevier,* Amsterdam, 351–368.

Li Ch. & Yang Sh. 2010: Is chemical index of alteration (CIA) a reliable proxy for chemical weathering in global drainage basins. *American Journal of Science* 510, 111–127.

Li F., Yan J., Chen Z.-Q., Ogg J.G., Tian L., Korngreen D., Liu K., Ma Z. & Woods A.D. 2015: Global oolite deposits across the Permian–Triassic boundary: a synthesis and implications for palaeoceanography immediately after the end-Permian biocrisis. *Earth-Sci. Rev.* 149, 163–180.

Li Y.-H. 2000: A compendium of geochemistry from solar nebula to rthe human brain. *Princeton University Press,* Princeton, 1–475.

Lin J., Li J. & Sun Q. 1990: Late Palaeozoic foraminifers in South China. *Science Publishing House*, Beijing, 1–297 (in Chinese with English abstract).

Lin R. 1979: Upper Permian fusulinids from western Guizhou. *Acta Palaeontol. Sinica* 18, 271–300.

Luo G., Wang Y., Algeo T.J., Kump L.R., Bai X., Yang H., Yao L. & Xie S. 2011. Enhanced nitrogen fixation in the immediate aftermath of the latest Permian marine mass extinction. *Geology* 39, 7, 647–650.

Miklukho-Maklay A.D. 1958: New family of foraminifers — Tuberitinidae M.-Maclay fam. nov. *Voprosy Mikropaleontologii* 2, 130–135 (in Russian).

Miklukho-Maklay K.V. 1954: Foraminifers from Upper Permian deposits of the northern Caucasus [Foraminifery verkhnepermskikh otlozheniy severnogo Kavkaza]. *Gosgeoltekhizdat*, Moskva, 1–163 (in Russian).

Nesbitt H.W. & Young G.M. 1982: Early Proterozoic climates and plate motions inferred from major element chemistry of lutites. *Nature* 199, 715–717.

Nesbitt H.W., Fedo C.M. & Young G.M. 1997: Quartz and Feldspar Stability, Steady and Non-Steady-State Weathering and Pedogenesis of Siliciclastics Sands and Muds. *J. Geol.* 105, 173–191.

Nestell G.P. & Nestell M.K. 2006: Middle Permian (Late Guadalupian) foraminifers from Dark Canyon, Guadalupe Mountains, New Mexico. *Micropaleontology* 52, 1–50.

Nestell G.P., Sudar M.N., Jovanović D. & Kolar-Jurkovšek T. 2009: Latest Permian foraminifers from the Vlašić mountain area, northwestern Serbia. *Micropaleontology* 55, 495–513.

Nestell G.P., Kolar-Jurkovšek T., Jurkovšek B. & Aljinović D. 2011: Foraminifera from the Permian–Triassic transition in western Slovenia. *Micropaleontology* 57, 197–222.

Nestell G.P., Nestell M.K., Ellwood B.B., Wardlaw B.R., Basu A.R., Ghosh N., Luu Thi Phuong Lan, Rowe H.D., Hunt A., Tomkin J.H. & Ratcliffe K.T. 2015: High influx of carbon in walls of agglutinated foraminifers during the Permian–Triassic transition in global oceans. *Int. Geol. Rev.* 57, 411–427.

Nicoll R.S., Metcalfe I. & Wang C.-Y. 2002: New species of the conodont Genus *Hindeodus* and the conodont biostratigraphy of the Permian–Triassic boundary interval. *J. Asian Earth Sci.* 20, 609–631.

Ogg J.G. 2012: Triassic. In: Gradstein F.M., Ogg J.G., Schmitz M.D. & Ogg. G.M. (Eds.): The Geologic Time Scale 2012. Volume 2. *Elsevier B.V.*, 681–730.

Patey M.D., Achterberg E.P., Rijkenberg M.J. & Pearce R. 2015: Aerosol time-series measurements over the tropical Northeast Atlantic Ocean: dust sources, elemental composition and mineralogy. *Mar. Chem.* 174, 103–119.

Pronina G.P. 1989: Foraminifers of the *Paratirolites kittli* Zone of the Dorashamian of the Late Permian of Transcaucasia [Foraminifery zony *Paratirolites kittli* dorashamskogo yarusa pozdney permi Zakavkaz'ya]. *Ezhegodnik Vsesoyuznogo Paleontologicheskogo obshchestva* 32, 30–36 (in Russian).

Pronina-Nestell G.P. & Nestell M.K. 2001: Late Changhsingian foraminifers of the Northwestern Caucasus. *Micropaleontology* 47, 205–234.

Quan T.M. & Falkowski P.G. 2009: Redox control of N: P ratios in aquatic ecosystems. *Geobiology* 7, 2, 124–139.

Reitlinger E.A. 1950: Foraminifera of the Middle Carboniferous deposits of the central part of the Russian Platform (exclusive of the family Fusulinidae). *Akademiya Nauk SSSR, Institut Geologicheskikh Nauk, Trudy* 126*, Geologicheskaya Seriya* 47, 1–126 (in Russian).

Sageman B.B. & Lyons T.W. 2005: Geochemistry of fine grained sediments and sedimentary rocks. In: MacKenzie F.T. (Ed): Sediments, diagenesis and sedimentary rocks. *Treatise on Geochemistry* 7, *Elsevier,* Amsterdam, 115–158.

Schobben M., Joachimski M.M., Korn D., Leda L. & Korte Ch. 2014: Palaeotethys seawater temperature rise and an intensified hydrological cycle following the end-Permian mass extinction. *Gondwana Res.* 26, 675–683.

Sellier de Civrieux J.M. & Dessauvagie T.F.J. 1965: Reclassification de quelques Nodosariidae, particulièrement du Permien au Lias. *Institut d'Études et de Recherches Minières de Turquie* 124, 1–178.

Song H., Tong J. & He W. 2006: Latest Permian foraminiferal fauna at the Meishan section, Zhejiang Province. *Acta Micropalaeontol. Sinica* 23, 87–104.

Song H., Tong J., Zhang K., Wang Q. & Chen Z.Q. 2007: Foraminiferal survivors from the Permian–Triassic mass extinction in the Meishan section, South China. *Palaeoworld* 16, 105–119.

Song H., Tong J., Chen Z.Q., Yang H. & Wang Y. 2009: End-Permian mass extinction of foraminifers in the Nanpanjing basin, South China. *J. Paleontology* 83, 718–738.

Sudar M., Jovanović D. & Kolar-Jurkovšek T. 2007: Late Permian conodonts from Jadar Block (Vardar Zone, northwestern Serbia). *Geol. Carpath.* 58, 2, 145–152.

Sudar M.N., Chen Yl., Kolar-Jurkovšek T., Jurkovšek B., Jovanović D. & Forel M.-B. 2014: Lower Triassic (Olenekian) microfauna from Jadar Block (Gučevo Mt., NW Serbia). *Geološki anali Balkanskoga poluostrva* (Beograd) 75, 1–15 (in English with Serbian summary).

Tribovillard N., Algeo T.J., Lyons T. & Riboulleau A. 2006: Trace metals as paleoredox and paleoproductivity proxies: an update. *Chem. Geol.* 232, 12–32.

Wang K. 1976: The Foraminifera from the Changhsing Formation in western Guizhou. *Acta Palaeontol. Sinica* 15, 187–196.

Wei G., Liu Y., Li X., Shao L., & Liang X. 2003: Climatic impact on Al, K, Sc and Ti in marine sediments: evidence from ODP Site 1144, South China Sea. *Geochem. J.* 37, 593–602.

Wignall P.B. & Myers K.J. 1988: Interpreting the benthic oxygen levels in mudrocks, a new approach. *Geology* 16, 452–455.

Williams J., Sudar M., Jovanović D. & Brookfield M.E. 2013a: Geochemistry and sedimentology of a new Permo–Triassic boundary section in Serbia. In: Zhong-Qiang Chen, Hao Yang & Genming Luo (Eds.): World summit on P–Tr mass extinction & extreme climate change (Wuhan, China, June 13-15, 2013), Abstracts. *State Key Laboratory of Biogeology and Environmental Geology, China University of Geosciences,* Wuhan, China, 78.

Williams J.C., Stebbins A., Sudar M., Jovanovic D., Brookfield M.E., Algeo T.J., Hannigan R. & Berman M. 2013b: The geochemistry of a newly discovered Permo–Triassic section in Serbia: A tale of catastrophic events. In: AGU Fall Meeting Abstracts. Abs. V33E-2815.

Williams J., Stebbins A., Sudar M.N., Jovanović D., Kolar-Jurkovšek T., Jurkovšek B., Brookfield M., Algeo T. & Hannigan R. 2014: Geochemistry of a new Permo–Triassic boundary section in Serbia. In: Proceedings of XX CBGA Congress, Tirana, Albania, 24–26 September 2014, General Session G02, 2/2014, Special Issue, 101.

Williford K.H., Foriel J., Ward P.D. & Steig E.J. 2009: Major perturbation in sulfur cycling at the Triassic–Jurassic boundary. *Geology* 37, 9, 835–838.

Yin H., Zhang K., Tong J., Yang Z. & Wu S. 2001: The Global Stratotype Section and Point (GSSP) of the Permian–Triassic Boundary. *Episodes* 24, 102–114.

Zhang Z. & Hong Z. 2004: Smaller foraminiferal fauna from the Changhsing Formation of Datian, Fujian. *Acta Micropalaeontol. Sinica* 21, 64–84.

Zhao J., Sheng J., Yao Z., Liang X., Chen C., Rui L. & Liao Z. 1981: The Changhsingian and Permian–Triassic boundary of South China. *Bulletin of Nanjing Institute of Geology and Palaeontology* 2, 1–112 (in Chinese with English abstract).

Zhou L., Wignall P.B., Su J., Feng Q., Xie Sh., Zhao L. & Huang J. 2012: U/Mo ratios and $\delta^{98/95}$Mo as local and global redox proxies during mass extinction events. *Chem. Geol.* 324–325, 99–107.